Geochemistry Geophysics Geosystems G3

Article
Volume 13, Number 1
20 January 2012
Q01013, doi:10.1029/2011GC003785
ISSN: 1525-2027

Published by AGU and the Geochemical Society

Distribution of major elements in Atlantic surface sediments (36°N–49°S): Imprint of terrigenous input and continental weathering

Aline Govin and Ulrike Holzwarth
MARUM–Center for Marine Environmental Sciences, University of Bremen, Leobener Strasse, D-28359 Bremen, Germany (aline.govin@uni-bremen.de)

David Heslop
Research School of Earth Sciences, Australian National University, Canberra, ACT 0200, Australia

Lara Ford Keeling
Texas A&M University–Corpus Christi, Corpus Christi, Texas 78412, USA

Matthias Zabel, Stefan Mulitza, and James A. Collins
MARUM–Center for Marine Environmental Sciences, University of Bremen, Leobener Strasse, D-28359 Bremen, Germany

Cristiano M. Chiessi
School of Arts, Sciences and Humanities, University of São Paulo, São Paulo 12227–010, Brazil

[1] Numerous studies use major element concentrations measured on continental margin sediments to reconstruct terrestrial climate variations. The choice and interpretation of climate proxies however differ from site to site. Here we map the concentrations of major elements (Ca, Fe, Al, Si, Ti, K) in Atlantic surface sediments (36°N–49°S) to assess the factors influencing the geochemistry of Atlantic hemipelagic sediments and the potential of elemental ratios to reconstruct different terrestrial climate regimes. High concentrations of terrigenous elements and low Ca concentrations along the African and South American margins reflect the dominance of terrigenous input in these regions. Single element concentrations and elemental ratios including Ca (e.g., Fe/Ca) are too sensitive to dilution effects (enhanced biological productivity, carbonate dissolution) to allow reliable reconstructions of terrestrial climate. Other elemental ratios reflect the composition of terrigenous material and mirror the climatic conditions within the continental catchment areas. The Atlantic distribution of Ti/Al supports its use as a proxy for eolian versus fluvial input in regions of dust deposition that are not affected by the input of mafic rock material. The spatial distributions of Al/Si and Fe/K reflect the relative input of intensively weathered material from humid regions versus slightly weathered particles from drier areas. High biogenic opal input however influences the Al/Si ratio. Fe/K is sensitive to the input of mafic material and the topography of Andean river drainage basins. Both ratios are suitable to reconstruct African and South American climatic zones characterized by different intensities of chemical weathering in well-understood environmental settings.

Components: 14,700 words, 5 figures, 3 tables.

Keywords: Atlantic surface sediments; terrigenous input; major elements.

Index Terms: 1051 Geochemistry: Sedimentary geochemistry; 1065 Geochemistry: Major and trace element geochemistry; 4924 Paleoceanography: Geochemical tracers.

Received 8 July 2011; **Revised** 4 October 2011; **Accepted** 11 December 2011; **Published** 20 January 2012.

Govin, A., U. Holzwarth, D. Heslop, L. Ford Keeling, M. Zabel, S. Mulitza, J. A. Collins, and C. M. Chiessi (2012), Distribution of major elements in Atlantic surface sediments (36°N–49°S): Imprint of terrigenous input and continental weathering, *Geochem. Geophys. Geosyst.*, *13*, Q01013, doi:10.1029/2011GC003785.

1. Introduction

[2] Terrigenous materials are transported into the oceans via fluvial and eolian pathways, which are both sensitive to climate changes [e.g., *Milliman and Meade*, 1983; *Miller and Russell*, 1992; *Rea*, 1994]. While changes in aridity, wind strength and direction modify the magnitude and composition of eolian input [e.g., *Rea*, 1994; *Engelstaedter et al.*, 2006], variations in sea level [*Milliman et al.*, 1975] and continental precipitation [*Milliman and Meade*, 1983; *Milliman and Syvitski*, 1992] alter the amount and path of fluvial sediments transported into the ocean.

[3] The Atlantic Ocean receives a significant amount of terrigenous material from the African and South American continents, of eolian [e.g., *Engelstaedter et al.*, 2006] and fluvial [e.g., *Peucker-Ehrenbrink*, 2009] origins. Several approaches have been applied to marine sediment cores to reconstruct past variations in terrigenous supply into the Atlantic. They are based on (1) the carbonate and opal-free terrigenous fraction [e.g., *Ruddiman and Janecek*, 1989; *deMenocal et al.*, 1993; *Tiedemann et al.*, 1994; *deMenocal et al.*, 2000], (2) grain-size analyses [e.g., *Sarnthein et al.*, 1981; *Rea*, 1994; *Ratmeyer et al.*, 1999; *Stuut et al.*, 2002; *Holz et al.*, 2004; *Mulitza et al.*, 2010], (3) reflectance [e.g., *Balsam et al.*, 1995; *Heslop et al.*, 2007; *Itambi et al.*, 2009], (4) magnetic techniques [e.g., *Bloemendal et al.*, 1992; *Frederichs et al.*, 1999; *Evans and Heller*, 2003; *Itambi et al.*, 2009], and (5) the distribution of clay minerals [e.g., *Petschick et al.*, 1996]. Additionally, a growing number of studies use the major element composition of marine sediment cores to trace changes in terrigenous input into the Atlantic [e.g., *Arz et al.*, 1999; *Peterson et al.*, 2000; *Yarincik et al.*, 2000; *Haug et al.*, 2001; *Zabel et al.*, 2001; *Adegbie et al.*, 2003; *Jaeschke et al.*, 2007; *Mulitza et al.*, 2008; *Tisserand et al.*, 2009]. This effort results from the recent development of X-ray fluorescence (XRF) core scanners that can obtain nondestructive, almost continuous and relatively fast measurements of the intensities of major elements directly at the surface of sediment cores.

[4] Numerous major-element based proxies have been developed and used to reconstruct terrestrial paleoclimate with partly controversial interpretations. The intensities (or number of counts) of terrestrial single elements have been used to trace the supply of terrestrial material to the ocean. For example, increased intensities of iron (Fe) and titanium (Ti) were interpreted as increased supplies of siliciclastic material of fluvial origin in the Cariaco Basin [*Peterson et al.*, 2000; *Haug et al.*, 2001] and at the mouth of the Plata River [*Chiessi et al.*, 2009]. *Bozzano et al.* [2002] however used increased proportions of Fe as a proxy for high Saharan and Sahelian dust deposition in sediments off Morocco. In nearby sites, *Kuhlmann et al.* [2004a] used high intensities of potassium (K) as an indicator of Moroccan fluvial input that reflects humid terrestrial conditions. Conversely, *Mulitza et al.* [2008] interpreted increased proportions of K off Senegal as increased eolian input to the ocean reflecting dry terrestrial conditions. The choice and climatic interpretation of single elements hence differ from site to site. In addition, dilution processes such as changes in marine biological productivity [e.g., *Bozzano et al.*, 2002] affect the interpretation of single element concentrations (see section 4.1).

[5] Insensitive to dilution effects, elemental ratios are more useful than single elements [e.g., *Weltje and Tjallingii*, 2008]. Among existing ratios, iron/calcium (Fe/Ca), titanium/calcium (Ti/Ca), titanium/aluminum (Ti/Al), iron/potassium (Fe/K) and aluminum/silicon (Al/Si) are the most commonly used for paleoclimate reconstructions. Fe and Ti are related to the siliciclastic components of the sediment and vary with the terrigenous fraction of the sediment [e.g., *Arz et al.*, 1998; *Jansen et al.*, 1998], whereas Ca often represents the carbonate content of the sediment [*Peterson et al.*, 2000; *Bozzano et al.*, 2002]. The Fe/Ca and Ti/Ca ratios have hence been used to trace changes in terrigenous input of mainly fluvial origin, particularly offshore Northeastern Brazil [*Arz et al.*, 1998, 1999; *Jaeschke et al.*, 2007] and Western Africa [*Adegbie et al.*, 2003; *Pierau et al.*, 2010].

[6] In marine sediments, the coarse sediment fractions are enriched in Ti [e.g., *Schütz and Rahn*,

1982; *Shiller*, 1982], while Al is mostly associated with fine-particle clay minerals [*Biscaye*, 1965]. A number of studies from the tropical Atlantic [*Boyle*, 1983; *Zabel et al.*, 1999; *Yarincik et al.*, 2000; *Jullien et al.*, 2007; *Tisserand et al.*, 2009] interpreted past Ti/Al changes to represent grain size variations, and hence fluctuations in trade wind intensity and eolian supply. Similarly, the Ti/Al variability was also understood in terms of the relative contribution of eolian versus fluvial input in the eastern Mediterranean Sea [*Lourens et al.*, 2001] and off Senegal [*Itambi et al.*, 2009].

[7] In tropical humid regions, high precipitation promotes intense chemical weathering of bedrocks (e.g., continental shields and tropical alluvial plains) [*Middelburg et al.*, 1988; *Driessen et al.*, 2001]. This results in the presence of highly weathered soils whose geochemical signature rich in Fe [*Driessen et al.*, 2001] is transferred to marine sediments by fluvial input. In marine sediments, K derives from potassium feldspar [*Zabel et al.*, 2001] or illite [*Yarincik et al.*, 2000], which are both characteristic of drier regions with low chemical weathering rates [*Zabel et al.*, 2001]. *Mulitza et al.* [2008] used the Fe/K ratio as a proxy for fluvial versus eolian input off Senegal, where high Fe/K values indicate an increased supply of Senegal River suspended material relative to dust deposition.

[8] In marine sediments, Si is contained in all clay minerals, in particular in quartz grains [*Moore and Dennen*, 1970]. Al is mostly associated in the sediment with fine-grained clay minerals [*Biscaye*, 1965], in particular with kaolinite, which is a product of intensive chemical weathering under wet conditions [*Bonatti and Gartner*, 1973]. Studies off Senegal [*Itambi et al.*, 2009], Mauritania [*Tisserand et al.*, 2009] and in the North Canary basin [*Moreno et al.*, 2001] interpreted Si/Al variations as changes in terrigenous quartz input related to wind strength fluctuations. In addition, *Chiessi et al.* [2010] used the Al/Si ratio as a proxy for the intensity of continental chemical weathering within the Plata River drainage basin. Similarly, *Mulitza et al.* [2008] showed a high correlation between the amount of fine material and the Al/Si ratio. They interpreted high Al/Si values as increased river suspension input relative to dust deposition in sediments off Senegal.

[9] The above examples illustrate the variety of climate indicators derived from major element concentrations (Fe, Ti, K) and ratios (Fe/Ca, Ti/Ca, Ti/Al, Fe/K, Al/Si) measured in marine sediments. Here we present bulk elemental compositions of a collection of 128 Atlantic surface sediment samples (36°N–49°S) that are influenced by a wide variety of continental climatic regimes and of source rocks and soils. The objectives of our study are twofold. First, we aim to elucidate the influence of terrigenous input on the geochemical composition of tropical and subtropical Atlantic surface sediments. We hence discuss the processes influencing the spatial distribution of major elements (Ca, Fe, Al, Si, Ti, K) in Atlantic surface sediments. Second, we assess the potential of elemental ratios (Fe/Ca, Ti/Ca, Ti/Al, Al/Si, Fe/K), commonly obtained from XRF core scanners as part of paleoclimate studies, to reconstruct changes in terrestrial climate conditions over Africa and South America.

2. Material and Methods

2.1. Environmental Setting

[10] The Atlantic Ocean is the Earth's oceanic basin receiving the highest dust deposition flux, accounting for up to 70% of the global oceanic budget [*Engelstaedter et al.*, 2006]. Dust particles deposited into the Atlantic Ocean (south of 40°N) originate from three main arid regions (the Sahara-Sahel, Namibia-Botswana and Patagonia-Argentinean Pampas) [*Prospero et al.*, 2002; *Mahowald et al.*, 2005] (Figure 1). The Sahara and Sahel in northern Africa constitute by far the most prominent source of dust [*Prospero et al.*, 2002] (Figure 1a). Dust particles are mainly produced in the Bodélé depression in Chad and the Mauritania-Mali region [*Middleton and Goudie*, 2001; *Engelstaedter et al.*, 2006]. They are transported westward, both at high altitudes (5–6 km) during boreal summer [*Caquineau et al.*, 2002; *Engelstaedter et al.*, 2006] by the Saharan Air Layer across the North Atlantic [*Prospero*, 1996] toward South America and the Caribbean Sea [*Prospero et al.*, 1981], and at lower altitudes (1.5–3 km) during boreal winter-spring [*Orange and Gac*, 1990; *Caquineau et al.*, 2002] by the northeast trade winds along the northwest African margin [*Chiapello et al.*, 1997; *Caquineau et al.*, 2002]. To a lesser extent, dust is produced in the arid regions of Namibia and Botswana in southern Africa, with maximum dust emissions between June and October [*Prospero et al.*, 2002; *Bryant*, 2003]. Southern African dust particles are carried northwestward by the southeast trade winds and deposited at relatively short distances along the Namibian and Angolan margins [*Prospero et al.*, 2002] (Figure 1a). In South America, dust is produced in Patagonia and the Argentinean Pampas and is transported eastward by the westerly winds,

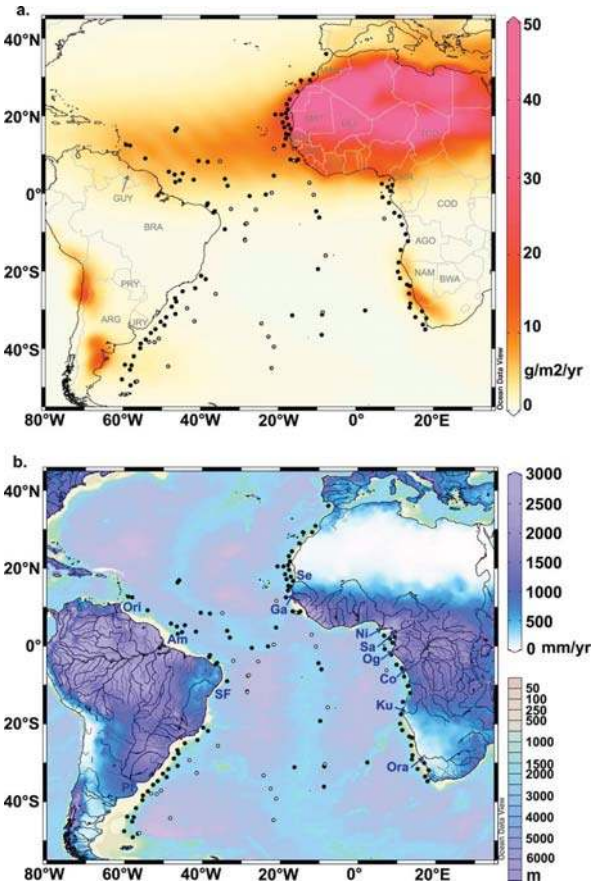

Figure 1. Sample locations. The black dots indicate the surface sediment samples located above the lysocline, while the white dots show the samples situated below the lysocline. (a) The dust deposition data (red scale) from *Mahowald et al.* [2005] show the extent of the dust plumes (red areas) originating from Northwestern Africa, Namibia and Patagonia. Country names mentioned in the text are indicated with gray letters following the ISO 3166 standard (AGO, Angola; ARG, Argentina; BRA, Brazil; BWA, Botswana; CIV, Ivory Coast; COD Democratic Republic of the Congo (Zaire); CMR, Cameroon; GIN, Guinea; GUY, Guyana; MAR, Morocco; MLI, Mali; MRT, Mauritania; NAM, Namibia; PRY, Paraguay; SEN, Senegal; TCD, Chad; URY, Uruguay). (b) The bathymetry (pastel scale in lower right corner) highlights the position of the mid-Atlantic ridge. Over the continents, the mean annual (1950–1999) terrestrial precipitation from the University of Delaware (http://climate.geog.udel.edu/~climate/) (blue scale in upper right corner), the major rivers (black line) and rivers of intermediate importance (gray line) are shown. Dark blue letters and arrows refer to the name and mouth of the main African Rivers (Se, Senegal; Ga, Gambia; Ni, Niger; Sa, Sanaga; Og, Ogooue; Co, Congo; Ku, Kunene; Ora, Orange) and South American Rivers (Ori, Orinoco; Am, Amazon; SF, São Francisco; Pl, Plata). The maps were generated with the Ocean Data View software [*Schlitzer*, 2010].

before settling into the South Atlantic south of 35°S [*Prospero et al.*, 2002] (Figure 1a).

[11] The main African and South American rivers (Figure 1b) rank among the world's largest [*Milliman and Meade*, 1983; *Milliman and Syvitski*, 1992; *Peucker-Ehrenbrink*, 2009]. Rivers with the highest runoff (i.e., the Amazon, Orinoco and Plata Rivers in South America; the Congo, Niger and Ogooue Rivers in Africa, Table 1) receive the highest amount of precipitation over their drainage basins [e.g., *Miller and Russell*, 1992; *Milliman and Syvitski*, 1992] (Figure 1b). The spatial distribution of precipitation is the primary factor controlling water discharge [*Milliman et al.*, 2008]. The size and topography of the drainage basin primarily control the sediment discharges of most rivers, while net precipitation and runoff play a secondary role [*Milliman and Syvitski*, 1992]. For example, the Orange River exhibits one of the highest sediment discharge values among the major African rivers, while its runoff remains very low (Table 1).

[12] The fate of riverine waters after their discharge in the coastal ocean has been investigated for some African and South American rivers. The development of a freshwater plume in the ocean does not only depend on the magnitude of the river discharge, but also on the direction and magnitude of the wind stress forcing [*Kourafalou et al.*, 1996]. For example, the southeast trade

Table 1. Drainage Basin Area, Annual Water Discharge and Annual Suspended Sediment Flux of the Main African and South American Rivers[a]

River	Drainage Basin Area (km^2)	Annual Water Discharge (km^3/yr)	Annual Suspended Sediment Flux (10^6 t/yr)
	Africa		
Senegal	353,000	21.9	2.2
Gambia	71,095	4.6	0.1
Niger	2,120,000	192.1	39.8
Sanaga	129,606	64.8	5.8
Ogooue	223,000	149.5	
Congo	3,710,000	1283.0	32.8
Kunene	108,250	6.8	0.4
Orange	945,000	11.4	88.8
	South America		
Orinoco	953,598	1100	173.2
Amazon	6,133,120	6300	1193.4
São Francisco	618,906	96	6.2
Plata	2,722,196	463.8	89.5

[a]From North To South. Values are the best estimates (usually the median of individual estimates) extracted from the recent compilation by *Peucker-Ehrenbrink* [2009].

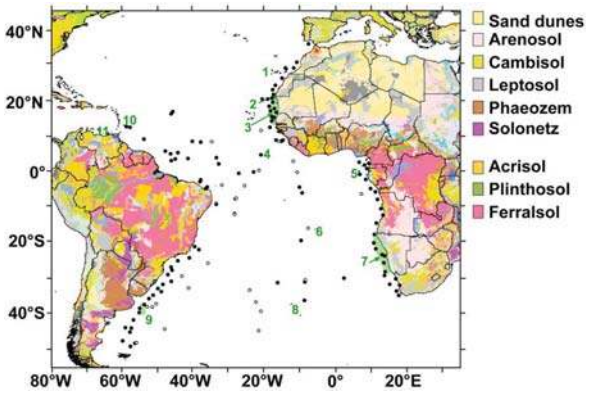

Figure 2. Major types of soils in Africa and South America [*FAO et al.*, 2009]. General soil characteristics are given in Table 2 (see *Driessen et al.* [2001] for a detailed description of the soil types). Intensively weathered soils (Acrisols, Plinthosols, Ferralsols) are observed in tropical humid areas, whereas slightly weathered soils (Sand dunes, Arenosols, Cambisols, Leptosols, Phaeozems, Solonetz) are present under drier conditions. The black dots indicate the samples located above the lysocline, while the white dots show the ones below the lysocline. Green numbers and shaded areas refer to specific geographic areas cited in the text: (1) Canary Islands, (2) Cape Blanc, (3) Mauritanian upwelling, (4) Sierra Leone Rise, (5) São Tomé island, (6) Santa Helena island, (7) Benguela upwelling, (8) Tristan da Cunha island, (9), Brazil-Malvinas Confluence, (10) Barbados islands and (11) the Cariaco Basin.

winds push the large plume of the Congo River offshore toward the north-northwest, forming a thin, low salinity surface layer [*Eisma et al.*, 1978]. Similarly, anomalously strong northeasterly winds blowing along the South American coast during El Niño conditions counteract the increased runoff of the Plata River induced by higher rainfall in the drainage basin and limit the northward penetration of the river plume along the Brazilian shelf observed under La Niña conditions [*Piola et al.*, 2005]. Off northern South America, most waters from the Amazon and Orinoco Rivers are directed northwestward toward the Caribbean Sea by the northeast trade winds [*Eisma et al.*, 1991; *Hu et al.*, 2004]. A significant part of the Amazon River plume is however deflected eastward into the North Equatorial Counter Current, in particular during Northern Hemisphere autumns (July–October) [*Muller-Karger et al.*, 1988, 1995; *Hu et al.*, 2004].

[13] Figure 2 shows the distribution of the major soil types in Africa and South America, the immediate sources for the terrigenous input to the Atlantic. Highly weathered soils, such as Acrisols, Plinthosols and Ferralsols (Table 2) (see *Driessen et al.* [2001] for a detailed description of the soil types), are predominantly observed in tropical African and South American regions (Figure 2) where annual rainfall is high (Figure 1b). In contrast, slightly weathered soils (e.g., sand dunes, Arenosols, Cambisols, Leptosols, Phaeozems and Solonetz [*Driessen et al.*, 2001]) (Table 2) are present at higher latitudes (Figure 2) in areas receiving less precipitation (Figure 1b). There is little information available on the geochemical composition of these different soil types. Intensively weathered soils are generally enriched in Fe and Al, whereas slightly weathered soils are relatively enriched in K and Si [*Moore and Dennen*, 1970; *Middelburg et al.*, 1988; *Driessen et al.*, 2001]. Relevant information on the elemental composition of eolian and fluvial material that originates from Africa and South America and deposits in the Atlantic is compiled in Table S3.[1]

2.2. Material

[14] To assess the factors influencing the modern geochemical composition of Atlantic sediments, we considered 128 sediment samples collected during 44 cruises of the German research vessels *Meteor*, *Poseidon* and *Sonne* over the last 25 years (Figure 1 and Table S1). We sampled the surface sediment of 3 giant box cores and 125 multicores. These devices limit the disturbance of surface sediments during the coring procedure. The samples are distributed in the South Atlantic and the tropical Atlantic between 36°N and 49°S (Figure 1 and Table S1). About 75% of the samples are located along the African and South American continental margins and 25% on the mid-Atlantic ridge or in the Atlantic abyssal basins (Figure 1). The water-depth of the samples ranges from 100 m to 5584 m. Most of the sites are presently located above the modern lysocline, i.e., shallower than 3500 m along the South American margin south of 30°S and shallower than 4000 m elsewhere [*Volbers and Henrich*, 2004] (Figure 1). Twenty-seven samples from the Atlantic abyssal basins are situated below the modern lysocline (Figure 1).

[15] We sampled the uppermost available sediment layer (0–0.5 cm, 0.5–1 cm or 0–1 cm) of

[1] Auxiliary materials are available in the HTML. doi:10.1029/2011GC003785.

Table 2. General Characteristics of Major Mineral Soil Types Shown in Figure 2[a]

Soil Type	Soil Formation Determined by a	Typical Environments	Main Distribution in Africa and South America	Degree of Weathering	General Soil Composition	Chemical Characteristics
Sand dunes	Sandy parent material	Active dunes	Sahara, Sahel	Very low	"non-soils" (sandy material)	
Arenosol	Sandy parent material	(Semi-) arid areas Inland dunes	Sahara, Sahel Central African plateau	Very low	Sandy soils rich in quartz and felspars	Rich in basic ions (e.g., Na, Ca, Mg, K)
Cambisol	Limited soil age	Temperate and boreal regions Active erosion	Andes (eastern Argentina) Eastern Paraguay	Moderate	Brown soils at an early stage of formation	Variable (presence of weatherable minerals)
Leptosol	Elevated and eroding environment	Mountain regions	Saharan desert Andes	Low	Very thin soils with highly variable composition	Highly variable
Phaeozem	Steppic climate	Wet steppe areas	Subtropical Argentinean and Uruguayan pampas	Moderate	Dark humus-rich soils	High organic content
Solonetz	(Semi-) arid climate	Areas with hot and dry summers	Western Paraguay Northern Argentina	Low	Dense clay natric (high proportion of adsorbed Na ions) soils	High Na and Mg contents
Acrisol	Wet (sub-) tropical climate	Humid acid rock erosional areas	Southern Amazon Basin Eastern (Ivory Coast) and western (Zaire) Africa	Intense	Strongly weathered acidic soils (rich in kaolinite)	High Fe and Al contents
Plinthosol	Wet (sub-) tropical climate	Rain forest areas Savannah zones	Eastern Amazon Basin Central Congo Basin	Intense	Iron-rich humus-poor mixture of kaolinitic clay and quartz	High Fe and Al contents
Ferralsol	Wet (sub-) tropical climate	Continental shields Alluvial lowlands	Brazilian, Zairian, Angolan and Guinean shields Amazon and Congo basins	Intense and deep	Clay assemblage dominated by kaolinite and hydrated Fe- and Al-oxides	High Fe and Al contents

[a]See *Driessen et al.* [2001] for detailed information. Country names are indicated in Figure 1a.

multicores, and used the 1–2 cm layer in only 13 samples (Table S1). Foraminiferal oxygen isotopic composition data and AMS ^{14}C dating in parallel piston, gravity cores and multicores [*Kuhlmann et al.*, 2004b; *Mollenhauer et al.*, 2004; *Seiter et al.*, 2005; *Chiessi et al.*, 2007] indicate a Holocene age for the used samples. Sedimentation rates are higher along the African coast and off the Northeastern Brazilian margin (sedimentation rate >5 cm/ka) than on the mid-Atlantic ridge or in the Atlantic abyssal basins (sedimentation rate down to 0.5 cm/ka) [*Kuhlmann et al.*, 2004b; *Mollenhauer et al.*, 2004; *Seiter et al.*, 2005]. The 0.5 cm- or 1 cm-thick surface sediment samples taken in this study therefore comprise a varying time-span ranging from a few decades in areas of high sedimentation to a maximum of 2000 years in regions with low sedimentation rates.

2.3. Measurement of Major Element Concentrations

[16] Sediment samples were stored at −20°C in the Bremen Core Repository (BCR, Germany). At room temperature, we sampled 3 to 6 mL of sediment (corresponding to 0.5 to 5 g of dry sediment) with cut syringes for geochemical analyses. Samples were freeze-dried, and then powdered and homogenized with an agate mortar. We chose to analyze the elemental concentrations of the bulk sediment rather than of the carbonate-free, opal-free and oxide-free fractions for one main reason. In order to assess the potential of elemental concentrations and ratios to reconstruct terrestrial climate zones, we wanted to measure the elemental composition of the sediment under similar conditions to the ones used by non-destructive XRF core scanning measurements, which are commonly applied in paleoclimate studies. Therefore we measured the concentration of major elements (Ca, Fe, Al, Si, Ti, K) of the bulk sediment samples by energy dispersive polarization X-ray Fluorescence (EDP-XRF) spectroscopy, using a SPECTRO XEPOS instrument [*Wien et al.*, 2005]. The device was operated with the software Spectro X-Lab Pro (Version 2.4), using the Turboquant method [*Schramm and Heckel*, 1998]. We assessed the analytical quality of the measurements by repeated analyses of the certified standard reference material MAG-1 [*Govindaraju*, 1994]. The measured values were within 1% of accepted values. The standard deviation of replicated sediment samples was less than 2%. The concentrations of major elements are expressed in grams per kilogram of dry sediment (g/kg). The concentration of K is below the detection limit (0.08 g/kg) in seven samples from the mid-Atlantic ridge (Table S1).

2.4. Cluster Analysis

[17] To identify characteristic groups of coherent elemental composition in Atlantic surface sediments, we performed a fuzzy c-means cluster analysis of the elemental data using the algorithm of *Bezdek* [1981]. We considered the concentrations of the five terrigenous elements Fe, Al, Si, Ti and K for the 96 samples located along the African and South American continental margins. The elemental data were pretreated using the *centered log-ratio* (clr) transform of *Aitchison* [1986] to map them from their simplicial sample space into a real space appropriate for cluster analysis [*Martín et al.*, 1998]. The fuzzy clustering employed Euclidean distances between the transformed data points and was calculated with a fuzzy exponent of 1.5. Each sample was assigned a membership in the interval [0,1] to each of the cluster centers, where a value of 1 indicates that a sample is identical to a cluster center (the membership value will decrease as the similarity with the cluster center decreases). For any given sample the total memberships over all the cluster centers must sum to unity. After the assignment of the memberships, the positions of the cluster centers were converted back to the original compositional data space using the inverse-clr [*Aitchison*, 1986].

3. Results

3.1. Distribution of Major Elements

[18] Figure 3 shows the distribution of major element concentrations in Atlantic surface sediments. We observe (1) very similar distributions of the terrigenous elements Al, Si, Fe, K, and Ti (Figures 3b–3f), and (2) a clearly opposite distribution of Ca (Figure 3a). Ca exhibits the highest concentrations on the mid-Atlantic ridge and the lowest concentrations along the African and South American margins (Figure 3a), in particular in areas close to the mouth of the Senegal, Gambia, Sanaga, Congo and Plata Rivers (see Figure 1b for the location of the rivers). The Ca distribution in the Atlantic surface sediments follows the modern distribution of Atlantic carbonate content [*Biscaye et al.*, 1976; *Balsam and McCoy*, 1987; *Archer*, 1996]. Most of the Ca contained in the Atlantic surface sediments can therefore be assigned to carbonates, most likely of marine origin, as shown by earlier studies [e.g., *Jansen et al.*, 1998; *Arz et al.*,

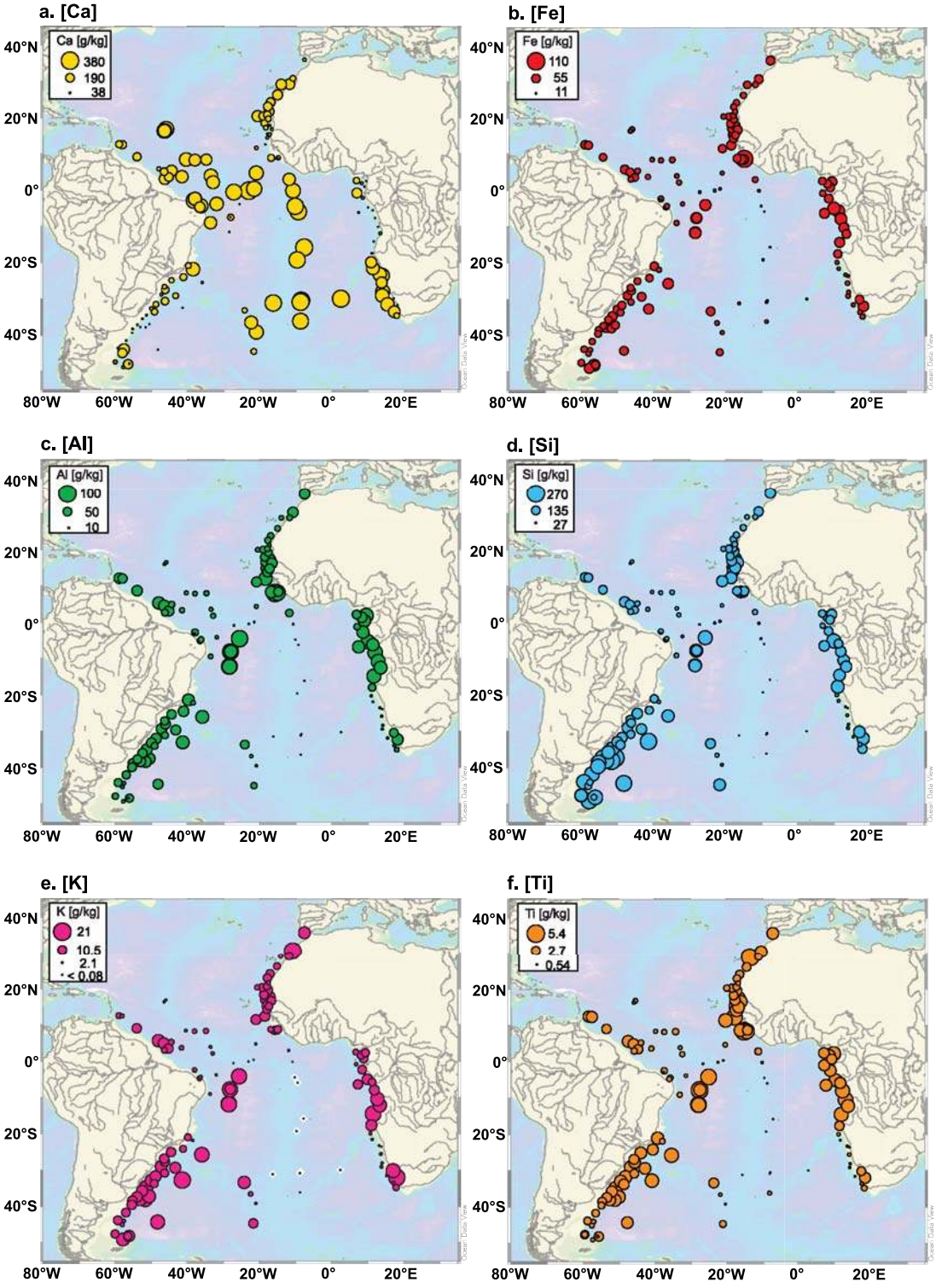

Figure 3. Spatial distribution of major element concentration (in g/kg) in Atlantic surface sediments (Table S1). Distribution of (a) Ca, (b) Fe, (c) Al, (d) Si, (e) K and (f) Ti. Black diamonds in (e) indicate samples for which the K concentration was below the detection limit (0.08 g/kg).

1999; *Richter et al.*, 2006; *Jullien et al.*, 2007; *Itambi et al.*, 2010]. In contrast, the concentrations of the five terrigenous elements are higher on the African and South American margins compared to the mid-Atlantic ridge (Figures 3b–3f). This pattern indicates a clear imprint of terrigenous input on the elemental composition of modern Atlantic surface sediments located on continental margins.

[19] The elemental distributions do not follow the above pattern in three distinct regions. We observe relatively high Ca concentrations and low concentrations of terrigenous elements (1) in African samples located between 19°S and 29°S off Namibia and (2) in samples off Northwest Africa between 18°N and 29°N (Figure 3). (3) We record extremely low Ca concentrations and high concentrations of terrigenous elements in eight samples (water-depth ranging from 4100 to 5600 m) distributed in the abyssal western Atlantic basin between 44°S and 4°S, parallel to the South American continent (Figure 3). Samples from these three particular regions indicate that factor other than the input of terrigenous material influence the geochemical composition of surface sediments on a regional scale (see section 4.1).

3.2. Distribution of Elemental Ratios

[20] Figure 4 shows the spatial distribution of the most commonly used elemental ratios Fe/Ca, Ti/Ca, Ti/Al, Fe/K and Al/Si. To account for the lack of symmetry exhibited by ratios, we present the logarithms of elemental ratios (see *Aitchison and Egozcue* [2005] for a review of the treatment of compositional data).

3.2.1. Distribution of Fe/Ca and Ti/Ca

[21] In Figures 4a–4b we show the Fe/Ca and Ti/Ca ratios of samples located above the lysocline (see section 4.1). As expected from the distributions of single elements (Figure 3), the Fe/Ca and Ti/Ca ratios present similar distributions (Figures 4a and 4b). Fe/Ca and Ti/Ca values are very low on the mid-Atlantic ridge and high along the continental margins, in particular in regions of high fluvial input from the Gambia, Sanaga, Congo, and Orange Rivers along Africa, and from the Orinoco, Amazon and Plata Rivers along South America (Figures 4a and 4b). We observe intermediate values on the mid-Atlantic ridge north of the equator (Figures 4a and 4b), i.e., in regions of high dust deposition [e.g., *Mahowald et al.*, 2005; *Chavagnac et al.*, 2008] (Figure 1a).

3.2.2. Distribution of Ti/Al

[22] Four sites located close to volcanic islands show high values Ti/Al compared to the main distribution (Figure 4c): (1) site GeoB5556–3 (29.3°N, 14.1°W) located to the north of the Canary Islands ($\ln(Ti/Al) = -1.55$), (2) site GeoB2019–2 (36.1°S, 8.8°W) from the eastern flank of the mid-Atlantic ridge to the east of the Tristan da Cunha island ($\ln(Ti/Al) = -1.69$), (3) site GeoB1412–2 (15.7°S, 7.8°W) located to the west of the Santa Helena island ($\ln(Ti/Al) = -2.50$), and (4) site GeoB4908–3 (0.7°S, 6.8°E) off Cameroon to the south of the São Tomé island ($\ln(Ti/Al) = -2.32$).

[23] Additionally, intermediate Ti/Al values (on average $\ln(Ti/Al)$ of -2.73 ± 0.09, 1σ standard deviation) are observed in (1) samples located off southern Brazil and Uruguay between 24°S and 38°S, (2) sites GeoB3936–2 and GeoB3939–1 off Barbados (ca. 12.5°N, 58.5°W) (see Figure 2 for the location of specific regions), (3) sites on the mid-Atlantic ridge to the north of 5°N, (4) site GeoB2910–2 (4.9°N, 21.1°W) on Sierra Leone Rise, (5) samples located off Northwestern Africa between 10°N and 25°N, and (6) sites located off Namibia at 18°S and 24°S (Figure 4c). With the exception of samples located along Southern Brazil and Uruguay, these sites are located in regions where the deposition of African eolian material dominates the terrigenous fraction [e.g., *Mahowald et al.*, 2005] (Figure 1a).

[24] Finally, the Ti/Al ratio exhibits low values ($\ln(Ti/Al) = -2.97 \pm 0.06$) at sites (1) located along the African margin between 9°N and 15°S (with the exception of site GeoB4908–3 next to the São Tomé island), and (2) along the South American margin of Northeastern Brazil and Guyana between 1°S and 10°N (Figure 4c). Both regions mainly receive terrigenous input of fluvial origin, from the Senegal [*Gac and Kane*, 1986], Niger [*Zabel et al.*, 2001] and Congo [*Eisma and van Bennekom*, 1978] Rivers on the one hand, and from the Amazon River [*Muller-Karger et al.*, 1988; *Zabel et al.*, 1999] on the other hand.

3.2.3. Distribution of Fe/K

[25] Figure 4d shows the distribution of the Fe/K ratio in Atlantic surface sediments. K concentrations below the detection limit in eight samples from the mid-Atlantic ridge (Figure 3e) explain the corresponding gap in the Fe/K distribution (Figure 4d). Similarly, very high Fe/K values ($\ln(Fe/K) > 2.00$) recorded in sites at 36°S and around the equator on

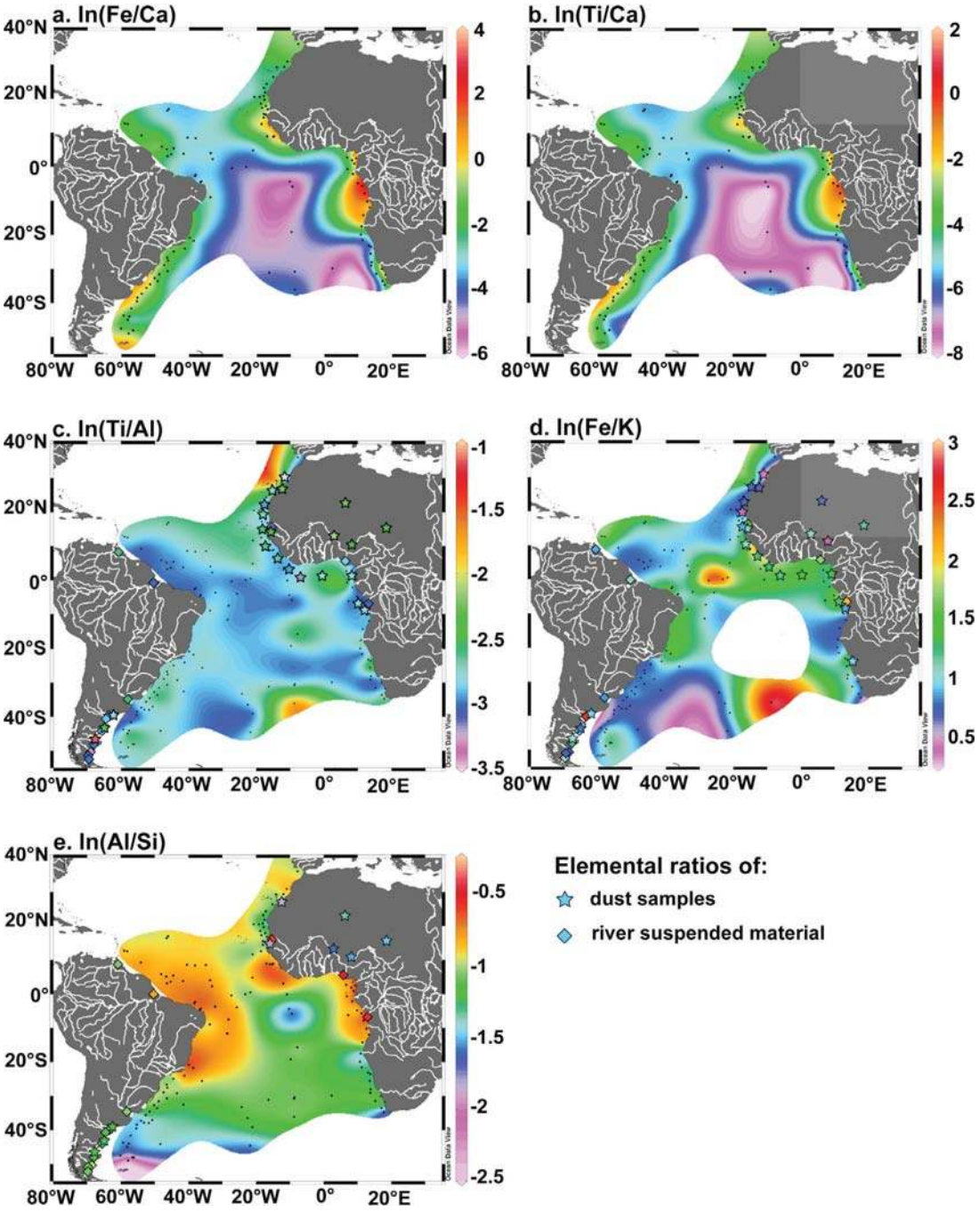

Figure 4. Spatial distribution of the ln-ratios of (a) Fe/Ca, (b) Ti/Ca, (c) Ti/Al, (d) Fe/K, and (e) Al/Si. The Fe/Ca and Ti/Ca ratios in panels (a) and (b) are shown for the samples located above the lysocline only. In panels (c), (d) and (e) are indicated the Ti/Al, Fe/K and Al/Si ratios of available sources: dust samples (stars) from North Africa [*Wilke et al.*, 1984; *Orange and Gac*, 1990; *Orange et al.*, 1993; *Stuut et al.*, 2005; *Moreno et al.*, 2006], Namibia [*Annegarn et al.*, 1983] and Patagonia [*Gaiero et al.*, 2007], as well as river suspended sediment (diamonds) from the Senegal [*Gac and Kane*, 1986], Niger [*Martin and Meybeck*, 1979; *Gaillardet et al.*, 1999], Congo [*Sholkovitz et al.*, 1978; *Martin and Meybeck*, 1979], Orinoco [*Hirst*, 1962; *Eisma et al.*, 1978; *Martin and Meybeck*, 1979], Amazon [*Sholkovitz et al.*, 1978; *Martin and Meybeck*, 1979], Plata [*Martin and Meybeck*, 1979; *Depetris et al.*, 2003] and Patagonian rivers [*Gaiero et al.*, 2007] (see Table S3 for details). The main South American and African rivers are shown in each panel. The maps were generated with the Ocean Data View software [*Schlitzer*, 2010].

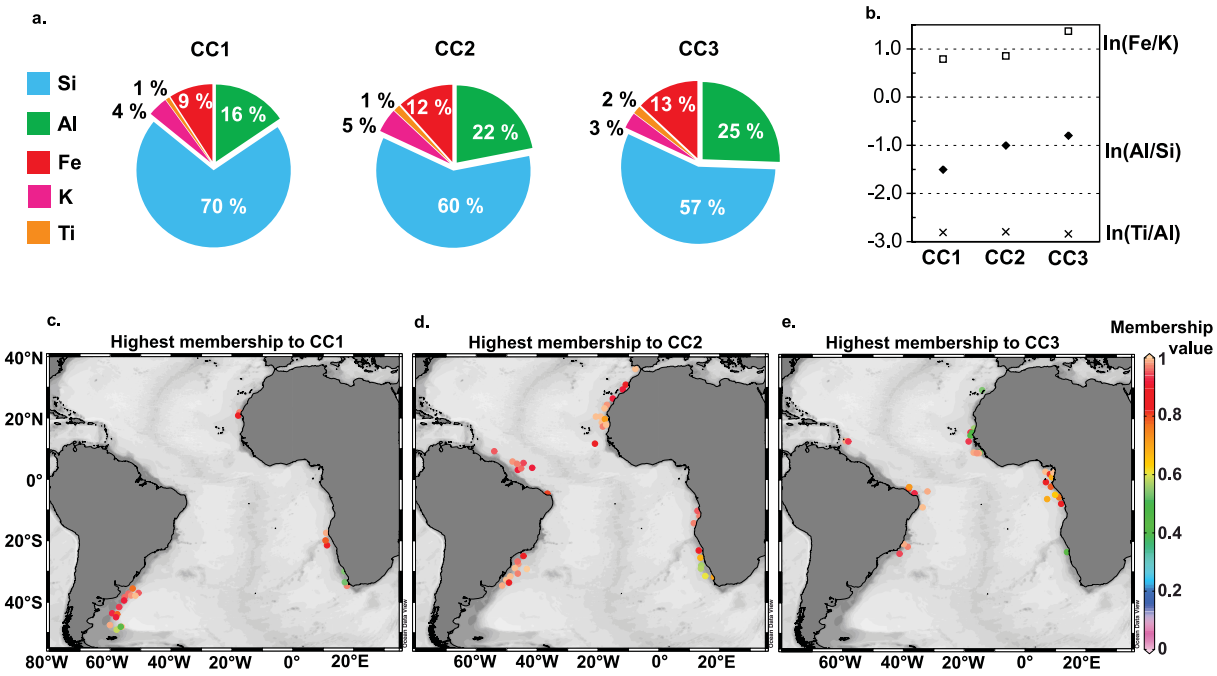

Figure 5. Results of the fuzzy c-means analysis, performed on the 96 samples located on the continental margins (see Table S2 for details). (a) Elemental composition (Si, Al, Fe, K, Ti) of cluster center 1 (CC1), cluster center 2 (CC2) and cluster center 3 (CC3). (b) Logarithm of elemental ratios (Fe/K, Al/Si and Ti/Al) of the three cluster centers. Spatial distribution of the membership values of samples to (c) CC1, (d) CC2, and (e) CC3. We only show the highest membership value of each sample to the cluster centers (see Table S2 for all values).

the mid-Atlantic ridge (Figure 4d) result from very low K concentrations in these samples (Figure 3e). Additionally, we record a high Fe/K ratio (ln(Fe/K) = 1.56) in site GeoB5556–3 (29.3°N, 14.1°W) located to north of the Canary Islands (Figure 4d), similar to the Ti/Al ratio at this site.

[26] Relatively high Fe/K values (ln(Fe/K) = 1.34 ± 0.32) are observed in continental margin samples from three tropical areas (Figure 4d): (1) in sites located along the African margin between 17°N and 8°S, i.e., in areas receiving strong fluvial input from the Senegal, Niger and Congo Rivers; (2) in sites located off Namibia between 23°S and 29°S, which receive terrigenous input from the Orange river; and (3) in samples located along the South American margin between 24°S and 12°N, with the exception of the samples in the vicinity of the Amazon River mouth. Conversely, the Fe/K distribution exhibits lower values (ln(Fe/K) = 0.83 ± 0.24) in drier regions (Figure 4d): (1) in samples located along the South American margin south of 24°S, and (2) in sites along the African margin north of 17°N and between 10°S and 22°S. Interestingly, we also record low Fe/K values in sites located closest to the Amazon mouth between 3°N and 10°N (ln(Fe/K) = 0.81 ± 0.05) (Figure 4d).

3.2.4. Distribution of Al/Si

[27] We observe high Al/Si values (ln(Al/Si) = −0.76 ± 0.11) in Atlantic surface sediments from tropical regions (Figure 4e): (1) along the African margin between 10°N and 15°S, and (2) along the South American margin between 12°N and 24°S. In contrast, intermediate Al/Si values (ln(Al/Si) = −1.16 ± 0.18) are found in drier regions: (1) along the African margin between 29°N and 10°N, (2) along the African margin between 15°S and 35°S, and (3) along the South American margin between 24°S and 35°S (Figure 4e). Finally, the Al/Si distribution exhibits low Al/Si values (ln(Al/Si) = −1.63 ± 0.30) in two distinct regions: (1) along the South American margin between 37°S and 49°S, and (2) in sites GeoB1612–9 (4.3°S, 10.3°W) and GeoB1808–7 (5.8°S, 9.4°W) from the mid-Atlantic ridge (Figure 4e).

3.3. Fuzzy c-means Cluster Analysis

[28] We present in Figure 5 the results of the fuzzy c-means cluster analysis performed on continental

margin samples (Table S2). We selected a solution with three cluster centers that highlight three groups with coherent geochemical compositions (Figure 5a). Samples located closest to Cape Blanc off Mauritania (19–22°N), along the Namibian and South African margins (17–35°S), at the mouth of the Plata River and further south along the Argentinean margin (35–49°S) demonstrate the highest membership to the first cluster center (CC1) (Figure 5c and Table S2). Across the suite of elements included in the cluster analysis, these samples contain low proportions of Al (16%), Fe (9%), K (4%) and Ti (1%) and a particularly high proportion of Si (70%) (Figure 5a).

[29] A lower proportion of Si (60%) and higher proportions of K (5%), Fe (12%) and Al (22%) characterize the second cluster center (CC2) (Figure 5a). Samples from Northwest Africa to the north of 17°N, off Angola (10°S-14°S), off Namibia and South Africa (23°S-32°S), close to the Amazon River mouth (3°N-9°N) and north of the Plata River mouth (24°S-35°S) show the highest membership to CC2 (Figure 5d and Table S2). These samples present coherent geochemical compositions characterized by intermediate Al/Si and low Fe/K values (Figure 5b). Located at subtropical latitudes, they mainly receive terrigenous input of fluvial origin for the South American margin and of eolian origin for the African margin (Figure 1). This cluster center indicates that similar geochemical compositions of sediment samples can reflect different environmental settings.

[30] The lowest proportions of Si (57%) and K (3%) and highest proportions of Al (25%) and Fe (13%) characterize the third cluster center (CC3) (Figure 5a). Samples located off the Canary Islands (ca. 29°N), off Africa between 17°N and 8°S, off Brazil between 3°S and 24°S and off Barbados islands (ca. 13°N) demonstrate the highest membership to CC3 (Figure 5e and Table S2). The highest Al/Si and Fe/K values characterize their elemental composition (Figure 5b). With the exception of site GeoB5556–3 near the Canary Islands, the samples with a highest membership to CC3 are located in Atlantic tropical regions, where the deposition of fluvial material dominates the sedimentation. Interestingly, samples located close to the Amazon River mouth do not exhibit the highest membership value to CC3 (Figure 5e). This cluster analysis nevertheless shows that tropical Atlantic surface sediments on the one hand, and subtropical surface sediments on the other hand, display distinct terrigenous compositions reflecting characteristic climatic regimes and soil types.

4. Discussion

4.1. Dilution Effects

[31] Elemental concentrations convey relative information on the geochemical composition of the sediment. Any variation in the concentration of one element will directly affect the concentration of other elements measured in the sediment. In our study we identify three processes that regionally induce such dilution effects: variations in the biological productivity of (1) carbonates, and of (2) biogenic opal, and (3) changes in carbonate dissolution. The potential dilution effect of (4) high organic carbon contents in Atlantic surface sediments is also discussed.

[32] 1. Sites from Northwest Africa and off Namibia display relatively high Ca concentrations and low concentrations of terrigenous elements for continental margin samples (Figure 3). They belong to the Mauritanian upwelling system [e.g., *Mittelstaedt*, 1983, 1991] and Benguela upwelling system [e.g., *Andrews and Hutchings*, 1980; *Nelson and Hutchings*, 1983]. In these regions, enhanced surface water biological productivity [e.g., *Bailey and Chapman*, 1991; *Van Camp et al.*, 1991] increases the deposition of carbonates on the seafloor [e.g., *Jahnke and Shimmield*, 1995] and the relative content of Ca in the sediment (Figure 3a).

[33] 2. The cluster analysis highlights the high proportion of Si (Figure 5a) at sites located along the Argentinean margin south of the Plata River mouth, off Cape Blanc, and along the Namibian and South African margin (Figure 5c). The African samples belong to the Benguela and Mauritanian upwelling systems [e.g., *Mittelstaedt*, 1983; *Nelson and Hutchings*, 1983]. These areas are characterized by a high biogenic opal production [e.g., *Bailey and Chapman*, 1991; *Romero et al.*, 2002], which explains the high Si concentrations and low Al/Si ratios of surface sediments. Moreover, the Al/Si ratio of sediments located along the Argentinean margin remains lower than that of any atmospheric dust and river suspended samples collected in Patagonia (Figure 4c and Table S3). This feature indicates the influence of external processes on the geochemical composition of Argentinean margin samples. These samples are located along the path of the Malvinas Current up to the Brazil-Malvinas Confluence, where the upper water

column is bathed by subantarctic water masses [e.g., *Gordon*, 1989; *Peterson and Stramma*, 1991]. They are hence located in a region of high siliceous productivity and receive strong input of biogenic opal [e.g., *Romero and Hensen*, 2002], explaining the very low Al/Si values. Similarly, the two samples from the mid-Atlantic ridge at ~5°S present high Si concentrations indicated by low Al/Si values (Figure 4e). Located in the equatorial Atlantic upwelling system, they also contain high proportions of biogenic opal [*Soldatov and Murdmaa*, 1970].

[34] 3. Samples from the abyssal southwestern Atlantic exhibit particularly low Ca concentrations and high concentrations of terrigenous elements for open ocean sites (Figure 3). With a water-depth ranging from 4100 to 5600 m, these sites are located below the modern lysocline [*Volbers and Henrich*, 2004] (Figure 1). Corrosive Antarctic Bottom Waters intensively dissolve carbonates deposited on the seafloor [*Volbers and Henrich*, 2004], leaving behind the terrigenous material and biogenic opal fractions.

[35] 4. *Mollenhauer et al.* [2004] document total organic carbon contents lower than 1% in most of South Atlantic surface sediments, with higher values up to 3% near the Plata and Congo River mouths and 10% in the Benguela upwelling system. High organic carbon contents have no influence on the elemental ratios considered in this study and could decrease the relative concentrations of measured single elements. We however do not observe any clear decrease in the single element concentrations in the Benguela upwelling region where the organic carbon content is the highest [*Mollenhauer et al.*, 2004]. This result suggests a negligible effect of organic carbon content on elemental distributions in the South Atlantic.

[36] Altogether, the potential influence of dilution and dissolution effects on the geochemical composition of the sediment prompt us to be cautious with the interpretation of elemental compositions used for paleoclimate reconstructions. First, the concentrations of single elements are interdependent and directly influenced by dilution effects. Therefore we do not recommend using the concentrations of single elements to reconstruct terrestrial paleoclimate. Less sensitive to dilution effects, elemental ratios are more useful [e.g., *Weltje and Tjallingii*, 2008]. Nevertheless, we note that elemental ratios including Ca (e.g., Fe/Ca, Ti/Ca) do not simply reflect the amount of terrigenous material deposited onto the seafloor. They rather reflect the amount of terrigenous input relative to the marine content. Because the concentration of Ca in the sediment depends on changes in marine carbonate productivity and dissolution, the application of these ratios to paleoclimate reconstructions requires a detailed understanding of the modern environmental setting and of its evolution during past climate changes.

4.2. Elemental Ratios as Proxies for Terrestrial Climate

4.2.1. Ti/Al, a Proxy for Eolian Versus Fluvial Input

[37] The distribution of Ti/Al in Atlantic surface sediments mainly shows intermediate Ti/Al values in areas of high dust deposition and low Ti/Al values in regions dominated by the input of suspended material from the Senegal, Niger, Congo and Amazon Rivers (Figure 4c and section 3.2.2). These results support the use of the Ti/Al ratio as a proxy for eolian versus fluvial terrigenous input [*Lourens et al.*, 2001; *Itambi et al.*, 2009]. High Ti/Al values indicate an increased contribution of dust input relative to the supply of river suspension matter.

[38] Available information on the geochemical composition of atmospheric dust and river suspended samples (Table S3) supports our interpretation of the Ti/Al ratio. Atmospheric dust samples collected along the West African coast between 25°N and 10°N [*Stuut et al.*, 2005], as well as dust samples from different North African regions [*Wilke et al.*, 1984; *Orange and Gac*, 1990; *Orange et al.*, 1993; *Moreno et al.*, 2006], exhibit intermediate Ti/Al values (Table 3 and Figure 4c). These values are similar to those measured in surface sediments from Northwestern Africa (10°N–25°N) and the tropical North Atlantic (Table 3 and Figure 4c), i.e., located below the dust plume [e.g., *Mahowald et al.*, 2005; *Chavagnac et al.*, 2008] (Figure 1a). In addition, suspended sediment from the Senegal [*Gac and Kane*, 1986], Niger [*Martin and Meybeck*, 1979; *Gaillardet et al.*, 1999] and Congo Rivers [*Sholkovitz et al.*, 1978; *Martin and Meybeck*, 1979] show low Ti/Al values (Table 3 and Figure 4c). These values are similar to those recorded in surface sediments from the tropical African margin (10°N–15°S) where fluvial input dominates (Table 3 and Figure 4c). Low Ti/Al values measured in Amazon River suspended material [*Sholkovitz et al.*, 1978; *Martin and Meybeck*, 1979] (Table 3 and Figure 4c) also agree with the Ti/Al values recorded along the North Brazilian and

Table 3. Summary of Elemental Ratio Values From (Left-Hand Side) Atlantic Surface Sediments Averaged for Specific Regions and (Right-Hand Side) Fluvial and Eolian Material of Relevant Sources[a]

Atlantic Surface Sediments		Available Sources		
Region	Mean ± 1SD	Region	Mean ± 1SD	Reference[b]
		ln(Ti/Al)		
North Africa (25°N–10°N), Sierra Leone, Barbados, mid-Atlantic ridge (>5°N)	−2.75 ± 0.07	North African dust (>6°N)	−2.60 ± 0.37	1
African tropical margin (10°N–15°S)	−2.96 ± 0.07	Senegal, Niger, Congo suspended matter	−3.03 ± 0.14	2
North Brazilian margin (10°N–5°S)	−2.98 ± 0.05	Amazon suspended matter	−3.03 ± 0.33	3
South Brazilian and Uruguayan margin (24°S–38°S)	−2.74 ± 0.07	Plata suspended matter	−2.56 ± 0.19	4
		ln(Fe/K)		
African margin: north of 17°N and south of 10°S	0.85 ± 0.25	North African (>10°N) and Namibian dust	0.77 ± 0.28	5
African tropical margin (17°N–10°S)	1.37 ± 0.33	Senegal, Niger, Congo suspended matter	1.79 ± 0.25	2
		Atmospheric dust along Africa (10°N–7°S)	1.30 ± 0.10	6
North Brazilian margin (10°N–3°N)	0.81 ± 0.05	Amazon suspended matter	1.09 ± 0.04	3
South Brazilian and Uruguayan margin (24°S–36°S)	0.79 ± 0.08	Plata suspended matter	0.85 ± 0.19	4
		ln(Al/Si)		
North African margin (>10°N)	−1.10 ± 0.15	North African dust	−1.63 ± 0.20	7
African tropical margin (10°N–15°S)	−0.75 ± 0.13	Senegal, Niger, Congo suspended matter	−0.57 ± 0.03	2
South American margin (12°N–24°S)	−0.77 ± 0.09	Amazon suspended matter	−0.81 ± 0.04	3
South Brazilian and Uruguayan margin (24°S–36°S)	−1.10 ± 0.11	Plata suspended matter	−1.07 ± 0.10	4

[a]See Table S3 details. We indicate the averaged ratio values ±1 standard deviation (SD) in log-space.
[b]References: 1 [*Wilke et al.*, 1984; *Orange and Gac*, 1990; *Orange et al.*, 1993; *Stuut et al.*, 2005; *Moreno et al.*, 2006]; 2 [*Sholkovitz et al.*, 1978; *Martin and Meybeck*, 1979; *Gac and Kane*, 1986; *Gaillardet et al.*, 1999]; 3 [*Sholkovitz et al.*, 1978; *Martin and Meybeck*, 1979]; 4 [*Martin and Meybeck*, 1979; *Depetris et al.*, 2003]; 5 [*Annegarn et al.*, 1983; *Wilke et al.*, 1984; *Orange and Gac*, 1990; *Orange et al.*, 1993; *Stuut et al.*, 2005; *Moreno et al.*, 2006]; 6 [*Stuut et al.*, 2005]; 7 [*Wilke et al.*, 1984; *Orange and Gac*, 1990; *Orange et al.*, 1993; *Moreno et al.*, 2006].

Guyanan margins between 10°N and 1°S (Table 3 and Figure 4c). This result supports the suggestion that Amazon suspended material constitutes the dominant source of terrigenous sediments in the western equatorial Atlantic, whereas North African dust deposition dominates on the eastern side of the mid-Atlantic ridge [*Zabel et al.*, 1999; *Abouchami and Zabel*, 2003].

[39] Suspended sediments from the Plata River exhibit intermediate Ti/Al values [*Martin and Meybeck*, 1979; *Depetris et al.*, 2003] (Table 3 and Figure 4c). These values are similar to the Ti/Al values recorded in surface sediments off south Brazil and Uruguay between 24°S and 38°S (Table 3 and Figure 4c). First, the extension of the Patagonian dust plume is limited to southernmost latitudes (Figure 1a). Second, most of the precipitation that falls over southern Brazil and Uruguay within the drainage basin of the Plata River is directed to the Plata River mouth, together with the relatively high load of suspended sediments (ca. 36°S) [e.g., *Depetris et al.*, 2003]. Fluvial material, which is transported northward from the Plata River mouth by a shelf coastal current [e.g., *Piola et al.*, 2005], therefore dominates the sedimentation along Uruguay and southern Brazil [e.g., *Frenz et al.*, 2004; *Mahiques et al.*, 2008]. The Ti/Al ratio of Plata River sediments however remains higher than that of the Senegal, Niger, Congo and Amazon Rivers (Table 3 and Figure 4c). Suspended sediments from the Plata River mostly derive from the mountainous drainage basin of the Bermejo River and other Andean tributaries. They carry the signature of young Andean volcanic rocks rich in Ti oxides, with some influence of the lowland Jurassic-Cretaceous tholeiithic basalts [*Depetris et al.*, 2003]. This feature explains why Ti/Al values in surface sediments off South Brazil and Uruguay are relatively high compared to those of other major rivers (Table 3 and Figure 4c). Moreover, it highlights the influence of terrigenous input with a mafic rock origin on the Ti/Al ratio of surface sediments. The high Ti/Al values measured in surface sediment samples located close to volcanic islands (Figure 4c and section 3.2.2) support this interpretation. Basaltic lava from the Canary [*Hoernle and Schmincke*, 1993; *Kuss and Kremling*, 1999], Tristan da Cunha [*Weaver et al.*, 1987], Santa Helena [*Weaver et al.*, 1987] and São Tomé [*Fitton and Dunlop*, 1985] islands are also enriched in Ti oxides.

[40] In summary, the Ti/Al ratio from Atlantic surface sediments records variations in the relative input of eolian (high Ti/Al) versus fluvial (low Ti/Al) terrigenous material, in areas of dust deposition and not affected by the input of mafic material. This corroborates the interpretation that increased Ti/Al values downcore in marine sediment cores represent an enhanced proportion of dust particles (versus reduced river suspended material) in regions of dust deposition. Past Ti/Al variations may also reflect changes in the provenance of terrigenous material (i.e., dominant watershed area) in a purely fluvial system [*Montero-Serrano et al.*, 2009, 2011].

4.2.2. Fe/K, a Tracer for Terrestrial Climatic Zones

[41] The Fe/K distribution along the Atlantic continental margins globally shows high values in African and Brazilian surface sediments from tropical areas and low Fe/K values in drier regions (Figures 4d and 5e and section 3.2.3). The geochemical composition of dust and river suspension samples from Africa supports this global pattern (Table 3, Figure 4d, and Table S3). A low Fe/K ratio characterizes dust particles collected at different places in North Africa [*Wilke et al.*, 1984; *Orange and Gac*, 1990; *Orange et al.*, 1993; *Moreno et al.*, 2006], off Northwestern Africa [*Stuut et al.*, 2005], off Angola [*Stuut et al.*, 2005], and in Namibia [*Annegarn et al.*, 1983] (Table 3 and Figure 4d). Their Fe/K values agree with those recorded in African margin surface sediments located north of 17°N and south of 10°S (Table 3 and Figure 4d), i.e., from relatively dry regions. In addition, low Fe/K values observed at subtropical latitudes in both dust particles and African surface sediments reflect the presence over Africa of slightly weathered soils relatively enriched in K [*Moore and Dennen*, 1970; *Middelburg et al.*, 1988; *Driessen et al.*, 2001] (Figure 2). These low Fe/K values indicate the dominant deposition of only slightly weathered particles originating from relatively dry areas on the subtropical African margin. Conversely, suspended material from the Senegal [*Gac and Kane*, 1986], Niger [*Martin and Meybeck*, 1979; *Gaillardet et al.*, 1999], and Congo River [*Sholkovitz et al.*, 1978; *Martin and Meybeck*, 1979] exhibits high Fe/K ratios (Table 3 and Figure 4d). These values are similar to those measured in tropical African sediments between 17°N and 10°S (Table 3 and Figure 4d), i.e., in regions of high fluvial sediment discharge (Table 1). In addition, the spatial Fe/K distribution observed along the African continental margin and in African dust and river suspended samples (Figure 4d) reflects the

spatial distribution of African soil types (Figure 2). High Fe/K values recorded in the tropics agree with the presence of intensively weathered soils (Ferralsols, Plinthosols, Acrisols) enriched in Fe over the adjacent continent [*Moore and Dennen*, 1970; *Middelburg et al.*, 1988; *Driessen et al.*, 2001] (Figure 2 and Table 2). Finally, atmospheric dust samples collected along the West African coast between 10°N and 7°S show higher Fe/K values than further north [*Stuut et al.*, 2005; *Mulitza et al.*, 2008] (Table 3 and Figure 4d). Increased Fe/K values of dust particles in the tropics reflect dust originating from highly weathered soils [*Chiapello et al.*, 1997; *Caquineau et al.*, 2002; *Moreno et al.*, 2006]. The deposition of such dust particles is likely to contribute to the high Fe/K values recorded in surface sediments from the tropical African margin. These high sedimentary Fe/K values reflect the fluvial or eolian input of intensively weathered material derived from tropical African regions. Altogether, the high similarity between the spatial distribution of Fe/K in African margin sediments and the distribution of African soil types indicates that terrigenous material deposited on continental margins is transported from the adjacent continent. In addition, the preceding comparison of Fe/K values recorded in African surface sediments and African terrigenous sources with the distribution of African soil types indicates that the Fe/K ratio in African margin sediments reflects the relative terrigenous input of highly weathered (mainly fluvial) material originating from tropical latitudes versus slightly weathered (eolian) material from subtropical latitudes.

[42] Surface sediments of two African arid regions reveal relatively high Fe/K values. First, north of the Canary Islands (GeoB5556–3, 29.3°N, 14.1°W), the high Fe/K value reflects the Fe-enriched signature of mafic rocks [*Hoernle and Schmincke*, 1993], in a manner similar to that described for the Ti/Al ratio (see section 4.2.1). This example highlights the sensitivity of the Fe/K ratio to terrigenous input of mafic material. Second, samples located along the Namibian and South African margin (between 23°S and 33°S) exhibit high Fe/K values for a dry region. These values reflect the input of Orange River suspended material and/or of dust particles that originate from inland dunes of the Namibian desert. Rich in iron, these dunes possess a distinctive reddish-brown color [*Scholz*, 1972; *Bremner and Willis*, 1993].

[43] High Fe/K values observed in South American continental margin samples from tropical areas (Figure 4d) reflect the presence of highly weathered soils in the tropical sector of South America (Figure 2), where annual rainfall is generally high (Figure 1b). The low Fe/K values determined between ca. 24°S and the mouth of the Plata River agree with low Fe/K values characteristic of suspended material from the Plata River [*Martin and Meybeck*, 1979; *Depetris et al.*, 2003] (Table 3 and Figure 4d), corroborating the suggested northward transport of the Plata River sedimentary plume [e.g., *Frenz et al.*, 2004; *Mahiques et al.*, 2008]. We cannot rule out the influence of mafic material (in a similar manner to the Ti/Al ratio) on the geochemical signature of Plata River suspended material. The input of mafic material would result in high Fe/K values, as is observed next to the Canary islands (Figure 4d). The low Fe/K values characterizing Plata River sediments more likely reflect the presence of illite-rich material derived from the mountainous drainage basin of the Bermejo River and other Andean tributaries, which drain moderately weathered soils [*Depetris and Griffin*, 1968; *Bertolino and Depetris*, 1992; *Depetris et al.*, 2003]. These results support the use of the Fe/K ratio to reconstruct South American climatic zones characterized by different degrees of chemical weathering.

[44] We observed particularly low Fe/K values in surface sediments affected by Amazon River input between 3°N and 10°N [e.g., *Zabel et al.*, 1999; *Abouchami and Zabel*, 2003] for a region of high sediment discharge (Figures 4d, 5d, and 5e). Low Fe/K values also characterize the suspension material from the Amazon River [*Sholkovitz et al.*, 1978; *Martin and Meybeck*, 1979], if compared to the Senegal [*Gac and Kane*, 1986], Niger [*Martin and Meybeck*, 1979; *Gaillardet et al.*, 1999] and Congo River [*Sholkovitz et al.*, 1978; *Martin and Meybeck*, 1979] sediments (Table 3 and Figure 4d). This feature of the Amazon River is surprising in the sense that intensively weathered soils (Ferralsols, Acrisols, Table 2) cover most of the lowland Amazon basin [*FAO et al.*, 2009] (Figure 2), which constitutes 88% of the entire drainage basin [*Guyot et al.*, 2007]. These low Fe/K values nevertheless agree with a high proportion of K related to a high illite content (30%) for tropical areas, recorded in nearby Atlantic surface sediments [*Biscaye*, 1965; *Petschick et al.*, 1996] and in suspended material from the Amazon River [*Guyot et al.*, 2007]. Due to the very strong rate of physical erosion in the Andes, the clay mineral composition of Andean rivers dominates that of Amazon suspended sediments, while the imprint of lowland rivers remains small [*Guyot et al.*, 2007]. Therefore, low Fe/K

values recorded in surface sediments between the Amazon River mouth and Guyana confirm the dominant Andean origin of Amazon suspended material on the one hand, and the dominant sedimentation of fluvial material in the western basin of the equatorial North Atlantic on the other hand. These values also indicate the influence of the topography of drainage basins on the geochemical composition of suspended material of large South American Rivers [*Milliman and Syvitski*, 1992]. This feature suggests the potential of the Fe/K ratio to reconstruct changes in the relative contribution of mountainous versus lowland sediment loads in Amazon suspended matter that deposits in the Atlantic.

[45] In summary, the Fe/K in surface sediments is suitable to reconstruct African and South American climatic zones, in areas not affected by the input of mafic material. The application of our results to paleoclimate reconstructions suggests that Fe/K values increasing downcore in marine sediments indicate the presence of more humid climatic conditions within the catchment area [*Mulitza et al.*, 2008]. Diagenetic Fe remobilization can however occur during redox processes in the sediment [e.g., *Middelburg et al.*, 1988; *Zwolsman and van Eck*, 1999] and bias paleoclimate reconstructions.

4.2.3. Al/Si, Another Tracer for Terrestrial Climatic Zones

[46] The Atlantic Al/Si distribution exhibits high values in continental margin samples from tropical areas and lower values in drier regions (Figures 4e, 5d, and 5e). The high Al/Si values form a tropical belt related to high kaolinite contents (>40%) in Atlantic surface sediments [*Biscaye*, 1965; *Petschick et al.*, 1996]. These values agree with the very high Al/Si values measured in suspended sediments from the Senegal [*Gac and Kane*, 1986], Niger [*Martin and Meybeck*, 1979; *Gaillardet et al.*, 1999] and Congo Rivers [*Sholkovitz et al.*, 1978; *Martin and Meybeck*, 1979] (Table 3 and Figure 4e), which drain highly weathered soils enriched in kaolinite (high Al content) [*Driessen et al.*, 2001; *FAO et al.*, 2009] (Figure 2). The distribution of Al/Si in tropical Atlantic sediments (Figure 4e) also shows high similarities to the African and South American distribution of intensively weathered soils (Figure 2). This result confirms the deposition on Atlantic continental margins of terrigenous material originating from the adjacent continent.

[47] Amazon suspended sediments [*Martin and Meybeck*, 1979; *Sholkovitz and Price*, 1980] exhibit lower Al/Si values than the tropical African rivers (Table 3 and Figure 4e). This feature highlights the influence of slightly chemically weathered material from Andean tributaries on Amazon clay mineral assemblages [*Guyot et al.*, 2007]. However, high Al/Si values observed along the South American margin north of 24°S (Figure 4e) reflect the high proportion of kaolinite in marine sediments adjacent to small tropical South American rivers [*Biscaye*, 1965]. Because of a reduced variety of pedogenic conditions in their drainage basins, small South American Rivers deliver sediments enriched in kaolinite compared to large rivers [*Biscaye*, 1965]. High Al/Si values in Atlantic surface sediments hence reflect the (fluvial) input of highly weathered material from tropical humid regions.

[48] Decreased Al/Si values measured in sediment samples from the south Brazilian and Uruguayan margins (24°S–36°S) agree with the elemental composition of the Plata River suspended matter [*Martin and Meybeck*, 1979; *Depetris et al.*, 2003] (Table 3 and Figure 4e). These Al/Si values trace the fluvial supply of less-weathered terrigenous material from the Plata River drainage basin with a strong contribution of the Bermejo River and other Andean tributaries [*Depetris and Griffin*, 1968; *Bertolino and Depetris*, 1992]. Finally, the relatively low Al/Si values recorded off Northwest Africa (north of 10°N) agree with the geochemical composition of North African dust particles [*Wilke et al.*, 1984; *Orange and Gac*, 1990; *Orange et al.*, 1993; *Moreno et al.*, 2006] (Table 3 and Figure 4e). These values reflect the eolian input of slightly weathered material from (semi-) arid regions.

[49] Therefore, in a manner similar to the Fe/K ratio, the Al/Si ratio measured in Atlantic surface sediments reflects the relative input of highly weathered material derived from tropical humid regions versus slightly weathered particles from drier areas. The ratio is thus suitable for reconstructing African and South American climatic zones characterized by different degrees of continental weathering. For paleoclimate reconstructions, Al/Si values increasing downcore in marine sediment cores will indicate wetter climatic conditions in the catchment area. In parallel, changes in the Al/Si ratio are linked to variations in the grain size of terrigenous material, with increasing Al/Si values being related to an increased amount of fluvial fine-grained material off Senegal [*Mulitza et al.*, 2008]. Recent data from the Amazon tributaries also indicate a clear inverse relationship between the Al/Si ratio and the grain size of suspended material [*Bouchez*

et al., 2011]. The Al/Si ratio is however not suitable for terrestrial reconstructions in environments subject to high biogenic opal productivity (see section 4.1).

5. Conclusions

[50] In this study, we mapped for the first time the concentrations of major elements (Ca, Fe, Al, Si, K, Ti) in surface sediments from the tropical and subtropical Atlantic (36°N–49°S). Our data set shows high concentrations of terrigenous elements and low concentrations of Ca along the African and South American margins, and the opposite situation on the mid-Atlantic ridge. This feature reflects the imprint of terrigenous input along the African and South American margins. However, factors other than the input of terrigenous material regionally influence the geochemical composition of Atlantic surface sediments. From the Atlantic distribution of single elements and the cluster analysis, we identify here (1) the dilution of terrigenous elements by carbonates and biogenic opal in regions of enhanced biological productivity and (2) the dissolution of carbonates at greater water-depths. Single element concentrations are sensitive to these effects. Similarly, elemental ratios including Ca (e.g., Fe/Ca and Ti/Ca) reflect the amount of terrigenous input relative to the marine content, which is affected by dilution and dissolution effects. They hence do not allow reliable reconstructions of terrestrial climate conditions, in particular for past climate changes. Insensitive to dilution effects, elemental ratios including terrigenous elements are more appropriate [e.g., *Weltje and Tjallingii*, 2008]. They reflect the relative variation of two terrigenous elements that can be associated with contrasting situations (e.g., dry versus humid conditions, physical versus chemical weathering).

[51] The cluster analysis shows that coherent terrigenous compositions characterize the sediments from tropical Atlantic regions on the one hand, and subtropical regions on the other hand, reflecting different climatic regimes and source soils. We compared the elemental composition of Atlantic surface sediments with that of relevant fluvial and eolian material. The geochemical composition of terrigenous material deposited in the ocean determines the elemental ratios (e.g., Ti/Al, Fe/K, Al/Si) of surface sediments. The composition of terrigenous material depends on its source (i.e., rock types, soil types and their degree of chemical weathering) and ultimately reflects the climate conditions within the catchment areas. The Atlantic distribution of the Ti/Al ratio supports its use as a proxy for eolian versus fluvial input of terrigenous material. However, our results highlight the sensitivity of Ti/Al to the input of mafic material. The distributions of the Fe/K and Al/Si ratios in Atlantic surface sediments are highly similar to those of major soil types in Africa and South America. This result indicates the deposition on Atlantic continental margins of terrigenous material originating from the adjacent continent. In addition, the Fe/K and Al/Si ratios of Atlantic sediments reflect the relative input of terrigenous material from climatic zones characterized by different degrees of chemical continental weathering. High values indicate the dominant input of highly weathered material derived from tropical humid regions, while low Fe/K and Al/Si values reflect the input of only slightly chemically weathered material formed under drier conditions. Therefore both ratios are suitable to reconstruct African and South American climatic zones. Other processes however regionally influence their distribution: enhanced input of biogenic opal for Al/Si, input of mafic rock material, topography of Andean river drainage basins and diagenetic Fe remobilization for Fe/K. The application of these ratios to climate reconstructions must take these factors into account.

[52] Our data set may serve as a basis for studies using major element concentrations in Atlantic sediment cores in order to reconstruct past variations in climatic conditions over Africa and South America.

Acknowledgments

[53] We thank Nathalie M. Mahowald for supplying the dust deposition data. We also thank Leticia Cotrim da Cunha for fruitful discussions and her help for handling the dust deposition data (Figure 1a), as well as K. Enneking and M. Klann for technical support. We acknowledge the chief scientists and vessel crew of the research cruises *Petr Kottsov* BENEFIT/1, *Meteor* M16/1, M16/2, M20/1, M20/2, M22/1, M23/1, M23/2, M23/3, M29/1, M29/2, M29/3, M34/1, M34/2, M34/3, M34/4, M37/1, M38/1, M38/2, M41/1, M41/3, M41/4, M42/4b, M45/1, M45/5a, M46/1, M46/2, M46/3, M46/4, M49/3, M49/4, M56/2, M57/1, M57/2, M58/1, M58/2, M65/1, M65/2, *Poseidon* PO272 and *Sonne* SO86 for collecting the sediment samples. We acknowledge the Geosciences Department of the University of Bremen and MARUM for supplying the samples. This work was funded through the DFG Research Center / Cluster of Excellence "The Ocean in the Earth System." We finally thank the editor and two anonymous reviewers for their constructive comments on the manuscript.

References

Abouchami, W., and M. Zabel (2003), Climate forcing of the Pb isotope record of terrigenous input into the equatorial Atlantic, *Earth Planet. Sci. Lett.*, *213*(3–4), 221–234, doi:10.1016/S0012-821X(03)00304-2.

Adegbie, A. T., R. R. Schneider, U. Röhl, and G. Wefer (2003), Glacial millennial-scale fluctuations in central African precipitation recorded in terrigenous sediment supply and freshwater signals offshore Cameroon, *Palaeogeogr. Palaeoclimatol. Palaeoecol.*, *197*(3–4), 323–333, doi:10.1016/S0031-0182(03)00474-7.

Aitchison, J. (1986), *The Statistical Analysis of Compositional Data*, Chapman and Hall, London.

Aitchison, J., and J. Egozcue (2005), Compositional data analysis: Where are we and where should we be heading?, *Math. Geol.*, *37*(7), 829–850, doi:10.1007/s11004-005-7383-7.

Andrews, W. R. H., and L. Hutchings (1980), Upwelling in the Southern Benguela Current, *Prog. Oceanogr.*, *9*(1), 1–81.

Annegarn, H. J., R. E. Van Grieken, D. M. Bibby, and F. Von Blottnitz (1983), Background aerosol composition in the namib desert, South West Africa (Namibia), *Atmos. Environ.*, *17*(10), 2045–2053.

Archer, D. E. (1996), An atlas of the distribution of calcium carbonate in sediments of the deep sea, *Global Biogeochem. Cycles*, *10*(1), 159–174, doi:10.1029/95GB03016.

Arz, H. W., J. Pätzold, and G. Wefer (1998), Correlated millennial-scale changes in surface hydrography and terrigenous sediment yield inferred from last-glacial marine deposits off northeastern Brazil, *Quat. Res.*, *50*(2), 157–166, doi:10.1006/qres.1998.1992.

Arz, H. W., J. Pätzold, and G. Wefer (1999), Climatic changes during the last deglaciation recorded in sediment cores from the northeastern Brazilian Continental Margin, *Geo Mar. Lett.*, *19*(3), 209–218, doi:10.1007/s003670050111.

Bailey, G. W., and P. Chapman (1991), Short-term variability during an anchor station study in the southern Benguela upwelling system: Chemical and physical oceanography, *Prog. Oceanogr.*, *28*(1–2), 9–37, doi:10.1016/0079-6611(91)90019-I.

Balsam, W. L., and F. W. McCoy Jr. (1987), Atlantic sediments: Glacial/interglacial comparisons, *Paleoceanography*, *2*(5), 531–542, doi:10.1029/PA002i005p00531.

Balsam, W. L., B. L. Otto-Bliesner, and B. C. Deaton (1995), Modern and Last Glacial Maximum eolian sedimentation patterns in the Atlantic Ocean interpreted from sediment iron oxide content, *Paleoceanography*, *10*(3), 493–507, doi:10.1029/95PA00421.

Bertolino, S. R., and P. J. Depetris (1992), Mineralogy of the clay-sized suspended load from headwater tributaries of the Parana River: Bermejo, Pilcomayo, and Paraguay rivers, in *Interactions of Biogeochemical Cycles in Aqueous Ecosystems*, edited by E. T. Degens et al., pp. 19–31, Univ. of Hamburg, Hamburg, Germany.

Bezdek, J. C. (1981), *Pattern Recognition With Fuzzy Objective Function Algorithms*, Kluwer Acad., New York.

Biscaye, P. E. (1965), Mineralogy and sedimentation of recent deep-sea clay in the Atlantic Ocean and adjacent seas and oceans, *Geol. Soc. Am. Bull.*, *76*(7), 803–832, doi:10.1130/0016-7606(1965)76[803:MASORD]2.0.CO;2.

Biscaye, P. E., V. Kolla, and K. K. Turekian (1976), Distribution of calcium carbonate in surface sediments of the Atlantic Ocean, *J. Geophys. Res.*, *81*(15), 2595–2603, doi:10.1029/JC081i015p02595.

Bloemendal, J., J. W. King, F. R. Hall, and S. J. Doh (1992), Rock magnetism of Late Neogene and Pleistocene deep-sea sediments: Relationship to sediment source, diagenetic processes, and sediment lithology, *J. Geophys. Res.*, *97*(B4), 4361–4375, doi:10.1029/91JB03068.

Bonatti, E., and S. Gartner (1973), Caribbean climate during Pleistocene ice ages, *Nature*, *244*(5418), 563–565, doi:10.1038/244563a0.

Bouchez, J., J. Gaillardet, C. France-Lanord, L. Maurice, and P. Dutra-Maia (2011), Grain size control of river suspended sediment geochemistry: Clues from Amazon River depth profiles, *Geochem. Geophys. Geosyst.*, *12*, Q03008, doi:10.1029/2010GC003380.

Boyle, E. A. (1983), Chemical accumulation variations under the Peru current during the past 130,000 years, *J. Geophys. Res.*, *88*(C12), 7667–7680, doi:10.1029/JC088iC12p07667.

Bozzano, G., H. Kuhlmann, and B. Alonso (2002), Storminess control over African dust input to the Moroccan Atlantic margin (NW Africa) at the time of maxima boreal summer insolation: A record of the last 220 kyr, *Palaeogeogr. Palaeoclimatol. Palaeoecol.*, *183*(1–2), 155–168, doi:10.1016/S0031-0182(01)00466-7.

Bremner, J. M., and J. P. Willis (1993), Mineralogy and geochemistry of the clay fraction of sediments from the Namibian continental margin and the adjacent hinterland, *Mar. Geol.*, *115*(1–2), 85–116, doi:10.1016/0025-3227(93)90076-8.

Bryant, R. G. (2003), Monitoring hydrological controls on dust emissions: Preliminary observations from Etosha Pan, Namibia, *Geogr. J.*, *169*(2), 131–141, doi:10.1111/1475-4959.04977.

Caquineau, S., A. Gaudichet, L. Gomes, and M. Legrand (2002), Mineralogy of Saharan dust transported over northwestern tropical Atlantic Ocean in relation to source regions, *J. Geophys. Res.*, *107*(D15), 4251, doi:10.1029/2000JD000247.

Chavagnac, V., M. Lair, J. A. Milton, A. Lloyd, I. W. Croudace, M. R. Palmer, D. R. H. Green, and G. A. Cherkashev (2008), Tracing dust input to the Mid-Atlantic Ridge between 14°45′N and 36°14′N: Geochemical and Sr isotope study, *Mar. Geol.*, *247*(3–4), 208–225, doi:10.1016/j.margeo.2007.09.003.

Chiapello, I., G. Bergametti, B. Chatenet, P. Bousquet, F. Dulac, and E. S. Soares (1997), Origins of African dust transported over the northeastern tropical Atlantic, *J. Geophys. Res.*, *102*(D12), 13,701–13,709, doi:10.1029/97JD00259.

Chiessi, C. M., S. Ulrich, S. Mulitza, J. Pätzold, and G. Wefer (2007), Signature of the Brazil-Malvinas Confluence (Argentine Basin) in the isotopic composition of planktonic foraminifera from surface sediments, *Mar. Micropaleontol.*, *64*(1–2), 52–66, doi:10.1016/j.marmicro.2007.02.002.

Chiessi, C. M., S. Mulitza, J. Pätzold, G. Wefer, and J. A. Marengo (2009), Possible impact of the Atlantic Multidecadal Oscillation on the South American summer monsoon, *Geophys. Res. Lett.*, *36*, L21707, doi:10.1029/2009GL039914.

Chiessi, C. M., S. Mulitza, J. Pätzold, and G. Wefer (2010), How different proxies record precipitation variability over southeastern South America, *IOP Conf. Ser.*, *9*(1), 012007.

deMenocal, P. B., W. F. Ruddiman, and E. M. Pokras (1993), Influences of high- and low-latitude processes on African terrestrial climate: Pleistocene eolian records from equatorial Atlantic Ocean Drilling Program Site 663, *Paleoceanography*, *8*(2), 209–242, doi:10.1029/93PA02688.

deMenocal, P. B., J. Ortiz, T. Guilderson, J. Adkins, M. Sarnthein, L. Baker, and M. Yarusinsky (2000), Abrupt onset and termination of the African Humid Period: Rapid climate responses to gradual insolation forcing, *Quat. Sci. Rev.*, *19*(1–5), 347–361.

Depetris, P. J., and J. J. Griffin (1968), Suspended load in the Rio de la Plata drainage basin, *Sedimentology*, *11*(1–2), 53–60, doi:10.1111/j.1365-3091.1968.tb00840.x.

Depetris, P. J., J.-L. Probst, A. I. Pasquini, and D. M. Gaiero (2003), The geochemical characteristics of the Paraná River suspended sediment load: An initial assessment, *Hydrol. Processes*, *17*(7), 1267–1277, doi:10.1002/hyp.1283.

Driessen, P., J. Deckers, O. Spaargaren, and F. Nachtergaele (2001), *Lecture Notes on the Major Soils of the World*, Food and Agric. Org., Rome.

Eisma, D., and A. J. van Bennekom (1978), The Zaire river and estuary and the Zaire outflow in the Atlantic Ocean, *Neth. J. Sea Res.*, *12*(3–4), 255–272, doi:10.1016/0077-7579(78)90030-3.

Eisma, D., S. J. Van Der Gaast, J. M. Martin, and A. J. Thomas (1978), Suspended matter and bottom deposits of the Orinoco delta: Turbidity, mineralogy and elementary composition, *Neth. J. Sea Res.*, *12*(2), 224–251, doi:10.1016/0077-7579(78)90007-8.

Eisma, D., P. G. E. F. Augustinus, and C. Alexander (1991), Recent and subrecent changes in the dispersal of Amazon mud, *Neth. J. Sea Res.*, *28*(3), 181–192, doi:10.1016/0077-7579(91)90016-T.

Engelstaedter, S., I. Tegen, and R. Washington (2006), North African dust emissions and transport, *Earth Sci. Rev.*, *79*(1–2), 73–100, doi:10.1016/j.earscirev.2006.06.004.

Evans, M., and F. Heller (2003), *Environmental Magnetism: Principles and Applications of Enviromagnetics*, Academic, Amsterdam.

FAO, IIASA, ISRIC, ISSCAS, and JRC (2009), Harmonized World Soil Database, version 1.1, http://www.iiasa.ac.at/Research/LUC/External-World-soil-database/HTML/, F. A. O., Rome.

Fitton, J. G., and H. M. Dunlop (1985), The Cameroon line, West Africa, and its bearing on the origin of oceanic and continental alkali basalt, *Earth Planet. Sci. Lett.*, *72*(1), 23–38, doi:10.1016/0012-821X(85)90114-1.

Frederichs, T., U. Bleil, K. Däumler, T. von Dobeneck, and A. M. Schmidt (1999), The magnetic view on the marine paleoenvironment: Parameters, techniques and potentials of rock magnetic studies as a key to paleoclimatic and paleoceanographic changes, in *Use of Proxies in Paleoceanography: Examples From the South Atlantic*, edited by H. Fischer and G. Wefer, pp. 575–599, Springer, Berlin, doi:10.1007/978-3-642-58646-0_24.

Frenz, M., R. Höppner, J.-B. W. Stuut, T. Wagner, and R. Henrich (2004), Surface sediment bulk geochemistry and grain-size composition related to the oceanic circulation along the South American continental margin in the southwest Atlantic, in *The South Atlantic in the Late Quaternary: Reconstruction of Material Budgets and Current Systems*, edited by G. Wefer, S. Mulitza, and V. Ratmeyer, pp. 347–373, Springer, Berlin, doi:10.1007/978-3-642-18917-3_17.

Gac, J. Y., and A. Kane (1986), Le fleuve Sénégal: I. Bilan hydrologique et flux continentaux de matières particulaires à l'embouchure, *Sci. Geol. Bull.*, *39*(1), 99–130.

Gaiero, D. M., F. Brunet, J.-L. Probst, and P. J. Depetris (2007), A uniform isotopic and chemical signature of dust exported from Patagonia: Rock sources and occurrence in southern environments, *Chem. Geol.*, *238*(1–2), 107–120, doi:10.1016/j.chemgeo.2006.11.003.

Gaillardet, J., B. Dupré, and C. J. Allègre (1999), Geochemistry of large river suspended sediments: Silicate weathering or recycling tracer?, *Geochim. Cosmochim. Acta*, *63*(23–24), 4037–4051, doi:10.1016/S0016-7037(99)00307-5.

Gordon, A. L. (1989), Brazil-Malvinas Confluence–1984, *Deep Sea Res., Part A*, *36*(3), 359–384, doi:10.1016/0198-0149(89)90042-3.

Govindaraju, K. (1994), 1994 Compilation of working values and sample description for 383 geostandards, *Geostand. Newsl.*, *18*, 1–158.

Guyot, J. L., J. M. Jouanneau, L. Soares, G. R. Boaventura, N. Maillet, and C. Lagane (2007), Clay mineral composition of river sediments in the Amazon Basin, *Catena*, *71*(2), 340–356, doi:10.1016/j.catena.2007.02.002.

Haug, G. H., K. A. Hughen, D. M. Sigman, L. C. Peterson, and U. Rohl (2001), Southward migration of the Intertropical Convergence Zone through the Holocene, *Science*, *293*(5533), 1304–1308, doi:10.1126/science.1059725.

Heslop, D., T. von Dobeneck, and M. Höcker (2007), Using non-negative matrix factorization in the "unmixing" of diffuse reflectance spectra, *Mar. Geol.*, *241*(1–4), 63–78, doi:10.1016/j.margeo.2007.03.004.

Hirst, D. M. (1962), The geochemistry of modern sediments from the Gulf of Paria–I The relationship between the mineralogy and the distribution of major elements, *Geochim. Cosmochim. Acta*, *26*(2), 309–334, doi:10.1016/0016-7037(62)90017-0.

Hoernle, K. A. J., and H.-U. Schmincke (1993), The petrology of the Tholeiites through Melilite Nephelinites on Gran Canaria, Canary Islands: Crystal fractionation, accumulation, and depths of melting, *J. Petrol.*, *34*(3), 573–597.

Holz, C., J.-B. W. Stuut, and R. Henrich (2004), Terrigenous sedimentation processes along the continental margin off NW Africa: Implications from grain-size analysis of seabed sediments, *Sedimentology*, *51*(5), 1145–1154, doi:10.1111/j.1365-3091.2004.00665.x.

Hu, C., E. T. Montgomery, R. W. Schmitt, and F. E. Muller-Karger (2004), The dispersal of the Amazon and Orinoco River water in the tropical Atlantic and Caribbean Sea: Observation from space and S-PALACE floats, *Deep Sea Res., Part II*, *51*(10–11), 1151–1171.

Itambi, A. C., T. von Dobeneck, S. Mulitza, T. Bickert, and D. Heslop (2009), Millennial-scale northwest African droughts related to Heinrich events and Dansgaard-Oeschger cycles: Evidence in marine sediments from offshore Senegal, *Paleoceanography*, *24*, PA1205, doi:10.1029/2007PA001570.

Itambi, A. C., T. von Dobeneck, and A. T. Adegbie (2010), Millennial-scale precipitation changes over Central Africa during the late Quaternary and Holocene: Evidence in sediments from the Gulf of Guinea, *J. Quat. Sci.*, *25*(3), 267–279, doi:10.1002/jqs.1306.

Jaeschke, A., C. Rühlemann, H. Arz, G. Heil, and G. Lohmann (2007), Coupling of millennial-scale changes in sea surface temperature and precipitation off northeastern Brazil with high-latitude climate shifts during the last glacial period, *Paleoceanography*, *22*, PA4206, doi:10.1029/2006PA001391.

Jahnke, R. A., and G. Shimmield (1995), Particle flux and its conversion to the sediment record: Coastal ocean upwelling systems, in *Upwelling in the Ocean: Modern Processes and Ancient Records*, edited by C. P. Summerhayes et al., pp. 83–100, Wiley, New York.

Jansen, J. H. F., S. J. Van der Gaast, B. Koster, and A. J. Vaars (1998), CORTEX, a shipboard XRF-scanner for element analyses in split sediment cores, *Mar. Geol.*, *151*(1–4), 143–153, doi:10.1016/S0025-3227(98)00074-7.

Jullien, E., et al. (2007), Low-latitude "dusty events" vs. high-latitude "icy Heinrich events", *Quat. Res.*, *68*(3), 379–386, doi:10.1016/j.yqres.2007.07.007.

Kourafalou, V. H., L.-Y. Oey, J. D. Wang, and T. N. Lee (1996), The fate of river discharge on the continental shelf 1. Modeling the river plume and the inner shelf coastal current, *J. Geophys. Res.*, *101*(C2), 3415–3434, doi:10.1029/95JC03024.

Kuhlmann, H., H. Meggers, T. Freudenthal, and G. Wefer (2004a), The transition of the monsoonal and the N Atlantic climate system off NW Africa during the Holocene, *Geophys. Res. Lett.*, *31*, L22204, doi:10.1029/2004GL021267.

Kuhlmann, H., T. Freudenthal, P. Helmke, and H. Meggers (2004b), Reconstruction of paleoceanography off NW Africa during the last 40,000 years: Influence of local and regional factors on sediment accumulation, *Mar. Geol.*, *207*(1–4), 209–224, doi:10.1016/j.margeo.2004.03.017.

Kuss, J., and K. Kremling (1999), Spatial variability of particle associated trace elements in near-surface waters of the North Atlantic (30°N/60°W to 60°N/2°W), derived by large volume sampling, *Mar. Chem.*, *68*(1–2), 71–86, doi:10.1016/S0304-4203(99)00066-3.

Lourens, L. J., R. Wehausen, and H. J. Brumsack (2001), Geological constraints on tidal dissipation and dynamical ellipticity of the Earth over the past three million years, *Nature*, *409*(6823), 1029–1033, doi:10.1038/35059062.

Mahiques, M. M., C. C. G. Tassinari, S. Marcolini, R. A. Violante, R. C. L. Figueira, I. C. A. da Silveira, L. Burone, and S. H. de Mello e Sousa (2008), Nd and Pb isotope signatures on the Southeastern South American upper margin: Implications for sediment transport and source rocks, *Mar. Geol.*, *250*(1–2), 51–63, doi:10.1016/j.margeo.2007.11.007.

Mahowald, N. M., A. R. Baker, G. Bergametti, N. Brooks, R. A. Duce, T. D. Jickells, N. Kubilay, J. M. Prospero, and I. Tegen (2005), Atmospheric global dust cycle and iron inputs to the ocean, *Global Biogeochem. Cycles*, *19*, GB4025, doi:10.1029/2004GB002402.

Martín, J. A., C. Barceló, and V. Pawlowsky (1998), Measures of difference for compositional data and hierarchical clustering methods, in *Proceedings of the Fourth Annual Conference of the International Association for Mathematical Geology*, edited by A. Buccianti, G. Nard, and R. Potenza, pp. 526–531, De Frede, Naples, Italy.

Martin, J.-M., and M. Meybeck (1979), Elemental mass-balance of material carried by major world rivers, *Mar. Chem.*, *7*(3), 173–206, doi:10.1016/0304-4203(79)90039-2.

Middelburg, J. J., C. H. van der Weijden, and J. R. W. Woittiez (1988), Chemical processes affecting the mobility of major, minor and trace elements during weathering of granitic rocks, *Chem. Geol.*, *68*(3–4), 253–273, doi:10.1016/0009-2541(88)90025-3.

Middleton, N. J., and A. S. Goudie (2001), Saharan dust: Sources and trajectories, *Trans. Inst. Br. Geogr.*, *26*(2), 165–181, doi:10.1111/1475-5661.00013.

Miller, J. R., and G. L. Russell (1992), The impact of global warming on river runoff, *J. Geophys. Res.*, *97*(D3), 2757–2764.

Milliman, J. D., and R. H. Meade (1983), World-wide delivery of river sediment to the oceans, *J. Geol.*, *91*(1), 1–21, doi:10.1086/628741.

Milliman, J. D., and J. P. M. Syvitski (1992), Geomorphic/tectonic control of sediment discharge to the ocean: The importance of small mountainous rivers, *J. Geol.*, *100*(5), 525–544, doi:10.1086/629606.

Milliman, J. D., C. P. Summerhayes, and H. T. Barretto (1975), Quaternary sedimentation on the Amazon continental margin: A model, *Geol. Soc. Am. Bull.*, *86*(5), 610–614, doi:10.1130/0016-7606(1975)86<610:QSOTAC>2.0.CO;2.

Milliman, J. D., K. L. Farnsworth, P. D. Jones, K. H. Xu, and L. C. Smith (2008), Climatic and anthropogenic factors affecting river discharge to the global ocean, 1951–2000, *Global Planet. Change*, *62*(3–4), 187–194, doi:10.1016/j.gloplacha.2008.03.001.

Mittelstaedt, E. (1983), The upwelling area off Northwest Africa–A description of phenomena related to coastal upwelling, *Prog. Oceanogr.*, *12*(3), 307–331, doi:10.1016/0079-6611(83)90012-5.

Mittelstaedt, E. (1991), The ocean boundary along the northwest African coast: Circulation and oceanographic properties at the sea surface, *Prog. Oceanogr.*, *26*(4), 307–355, doi:10.1016/0079-6611(91)90011-A.

Mollenhauer, G., R. R. Schneider, T. Jennerjahn, P. J. Müller, and G. Wefer (2004), Organic carbon accumulation in the South Atlantic Ocean: Its modern, mid-Holocene and last glacial distribution, *Global Planet. Change*, *40*(3–4), 249–266, doi:10.1016/j.gloplacha.2003.08.002.

Montero-Serrano, J. C., V. Bout-Roumazeilles, N. Tribovillard, T. Sionneau, A. Riboulleau, A. Bory, and B. Flower (2009), Sedimentary evidence of deglacial megafloods in the northern Gulf of Mexico (Pigmy Basin), *Quat. Sci. Rev.*, *28*(27–28), 3333–3347, doi:10.1016/j.quascirev.2009.09.011.

Montero-Serrano, J.-C., et al. (2011), Contrasting rainfall patterns over North America during the Holocene and Last Interglacial as recorded by sediments of the northern Gulf of Mexico, *Geophys. Res. Lett.*, *38*, L14709, doi:10.1029/2011GL048194.

Moore, B. R., and W. H. Dennen (1970), A geochemical trend in silicon-aluminum-iron ratios and the classification of clastic sediments, *J. Sediment. Res.*, *40*(4), 1147–1152.

Moreno, A., J. Targarona, J. Henderiks, M. Canals, T. Freudenthal, and H. Meggers (2001), Orbital forcing of dust supply to the North Canary Basin over the last 250 kyr, *Quat. Sci. Rev.*, *20*(12), 1327–1339, doi:10.1016/S0277-3791(00)00184-0.

Moreno, T., X. Querol, S. Castillo, A. Alastuey, E. Cuevas, L. Herrmann, M. Mounkaila, J. Elvira, and W. Gibbons (2006), Geochemical variations in aeolian mineral particles from the Sahara-Sahel Dust Corridor, *Chemosphere*, *65*(2), 261–270, doi:10.1016/j.chemosphere.2006.02.052.

Mulitza, S., M. Prange, J.-B. W. Stuut, M. Zabel, T. von Dobeneck, A. C. Itambi, J. Nizou, M. Schulz, and G. Wefer (2008), Sahel megadroughts triggered by glacial slowdowns of Atlantic meridional overturning, *Paleoceanography*, *23*, PA4206, doi:10.1029/2008PA001637.

Mulitza, S., et al. (2010), Increase in African dust flux at the onset of commercial agriculture in the Sahel region, *Nature*, *466*(7303), 226–228, doi:10.1038/nature09213.

Muller-Karger, F. E., C. R. McClain, and P. L. Richardson (1988), The dispersal of the Amazon's water, *Nature*, *333*(6168), 56–59, doi:10.1038/333056a0.

Muller-Karger, F. E., P. L. Richardson, and D. McGillicuddy (1995), On the offshore dispersal of the Amazon's Plume in the North Atlantic: Comments on the paper by A. Longhurst, "Seasonal cooling and blooming in tropical oceans, *Deep Sea Res., Part I*, *42*(11–12), 2127–2137, doi:10.1016/0967-0637(95)00085-2.

Nelson, G., and L. Hutchings (1983), The Benguela upwelling area, *Prog. Oceanogr.*, *12*(3), 333–356, doi:10.1016/0079-6611(83)90013-7.

Orange, D., and J. Y. Gac (1990), Bilan géochimique des apports atmosphériques en domaines sahélien et soudano-

guinéen d'Afrique de l'Ouest (bassins supérieurs du Sénégal et de la Gambie), *Geodynamique*, *5*(1), 51–65.

Orange, D., J. Y. Gac, and M. J. Diallo (1993), Geochemical assessment of atmospheric deposition including Harmattan dust in continental West Africa, in *Tracers in Hydrology: Proceedings of an International Symposium Held at Yokohama, Japan, 21–23 July, 1993*, edited by N. E. Peters et al., *IAHS Publ.*, *215*, 303–312.

Peterson, L. C., G. H. Haug, K. A. Hughen, and U. Rohl (2000), Rapid changes in the hydrologic cycle of the tropical Atlantic during the last glacial, *Science*, *290*(5498), 1947–1951, doi:10.1126/science.290.5498.1947.

Peterson, R. G., and L. Stramma (1991), Upper-level circulation in the South Atlantic Ocean, *Prog. Oceanogr.*, *26*(1), 1–73, doi:10.1016/0079-6611(91)90006-8.

Petschick, R., G. Kuhn, and F. Gingele (1996), Clay mineral distribution in surface sediments of the South Atlantic: Sources, transport, and relation to oceanography, *Mar. Geol.*, *130*(3–4), 203–229, doi:10.1016/0025-3227(95)00148-4.

Peucker-Ehrenbrink, B. (2009), Land2Sea database of river drainage basin sizes, annual water discharges, and suspended sediment fluxes, *Geochem. Geophys. Geosyst.*, *10*, Q06014, doi:10.1029/2008GC002356.

Pierau, R., T. J. J. Hanebuth, S. Krastel, and R. Henrich (2010), Late Quaternary climatic events and sea-level changes recorded by turbidite activity, Dakar Canyon, NW Africa, *Quat. Res.*, *73*(2), 385–392, doi:10.1016/j.yqres.2009.07.010.

Piola, A. R., R. P. Matano, E. D. Palma, O. O. Möller Jr., and E. J. D. Campos (2005), The influence of the Plata River discharge on the western South Atlantic shelf, *Geophys. Res. Lett.*, *32*, L01603, doi:10.1029/2004GL021638.

Prospero, J. M. (1996), The atmospheric transport of particles to the ocean, in *Particle Flux in the Ocean*, edited by V. Ittekkot et al., pp. 19–53, John Wiley, New York.

Prospero, J. M., R. A. Glaccum, and R. T. Nees (1981), Atmospheric transport of soil dust from Africa to South America, *Nature*, *289*(5798), 570–572, doi:10.1038/289570a0.

Prospero, J. M., P. Ginoux, O. Torres, S. E. Nicholson, and T. E. Gill (2002), Environmental characterization of global sources of atmospheric soil dust identified with the NIMBUS 7 Total Ozone Mapping Spectrometer (TOMS) absorbing aerosol product, *Rev. Geophys.*, *40*(1), 1002, doi:10.1029/2000RG000095.

Ratmeyer, V., G. Fischer, and G. Wefer (1999), Lithogenic particle fluxes and grain size distributions in the deep ocean off northwest Africa: Implications for seasonal changes of aeolian dust input and downward transport, *Deep Sea Res., Part I*, *46*(8), 1289–1337, doi:10.1016/S0967-0637(99)00008-4.

Rea, D. K. (1994), The paleoclimatic record provided by eolian deposition in the deep sea: The geologic history of wind, *Rev. Geophys.*, *32*(2), 159–195, doi:10.1029/93RG03257.

Richter, T. O., S. Van der Gaast, B. Koster, A. Vaars, R. Gieles, H. C. De Stigter, H. De Haas, and T. C. E. van Weering (2006), The Avaatech XRF Core Scanner: Technical description and applications to NE Atlantic sediments, in *New Techniques in Sediment Core Analysis*, edited by R. G. Rothwell, *Geol. Soc. Spec. Publ.*, *267*, 39–50, doi:10.1144/GSL.SP.2006.267.01.03.

Romero, O. E., and C. Hensen (2002), Oceanographic control of biogenic opal and diatoms in surface sediments of the Southwestern Atlantic, *Mar. Geol.*, *186*(3–4), 263–280, doi:10.1016/S0025-3227(02)00210-4.

Romero, O. E., C. B. Lange, and G. Wefer (2002), Interannual variability (1988–1991) of siliceous phytoplankton fluxes off northwest Africa, *J. Plankton Res.*, *24*(10), 1035–1046, doi:10.1093/plankt/24.10.1035.

Ruddiman, W. F., and T. R. Janecek (1989), Pliocene-Pleistocene biogenic and terrigenous fluxes at equatorial Atlantic sites 662, 663, and 664, *Proc. Ocean Drill. Program Sci. Results*, *108*, 211–240.

Sarnthein, M., G. Tetzlaff, B. Koopmann, K. Wolter, and U. Pflaumann (1981), Glacial and interglacial wind regimes over the eastern subtropical Atlantic and North-West Africa, *Nature*, *293*(5829), 193–196, doi:10.1038/293193a0.

Schlitzer, R. (2010), Ocean Data View, software, Alfred Wegener Inst., Bremerhaven, Germany. [Available at http://odv.awi.de.]

Scholz, H. (1972), The soils in the central Namib Desert with special consideration of the soils in the vicinity of Gobabeb, *Madoqua*, *1*, 33–51.

Schramm, R., and J. Heckel (1998), Fast analysis of traces and major elements with ED(P)XRF using polarized X-rays: TURBOQUANT, *J. Phys. IV Fr.*, *8*(PR5), 335–342.

Schütz, L., and K. A. Rahn (1982), Trace-element concentrations in erodible soils, *Atmos. Environ.*, *16*(1), 171–176.

Seiter, K., C. Hensen, and M. Zabel (2005), Benthic carbon mineralization on a global scale, *Global Biogeochem. Cycles*, *19*, GB1010, doi:10.1029/2004GB002225.

Shiller, A. M. (1982), The geochemistry of particulate major elements in Santa Barbara Basin and observations on the calcium carbonate-carbon dioxide system in the ocean, PhD thesis, 197 pp., Univ. of California, San Diego.

Sholkovitz, E. R., and N. B. Price (1980), The major-element chemistry of suspended matter in the Amazon Estuary, *Geochim. Cosmochim. Acta*, *44*(2), 163–171, doi:10.1016/0016-7037(80)90128-3.

Sholkovitz, E. R., R. van Grieken, and D. Eisma (1978), The major-element composition of suspended matter in the Zaire river and estuary, *Neth. J. Sea Res.*, *12*(3–4), 407–413, doi:10.1016/0077-7579(78)90042-X.

Soldatov, A. V., and I. O. Murdmaa (1970), The mineral composition of the deposits in the Romanche gap, *Oceanology*, Engl. Transl., *10*, 375–381.

Stuut, J.-B. W., M. A. Prins, R. R. Schneider, G. J. Weltje, J. H. F. Jansen, and G. Postma (2002), A 300-kyr record of aridity and wind strength in southwestern Africa: Inferences from grain-size distributions of sediments on Walvis Ridge, SE Atlantic, *Mar. Geol.*, *180*(1–4), 221–233, doi:10.1016/S0025-3227(01)00215-8.

Stuut, J.-B. W., M. Zabel, V. Ratmeyer, P. Helmke, E. Schefuß, G. Lavik, and R. Schneider (2005), Provenance of present-day eolian dust collected off NW Africa, *J. Geophys. Res.*, *110*, D04202, doi:10.1029/2004JD005161.

Tiedemann, R., M. Sarnthein, and N. J. Shackleton (1994), Astronomic timescale for the Pliocene Atlantic $\delta^{18}O$ and dust flux records of Ocean Drilling Program Site 659, *Paleoceanography*, *9*(4), 619–638, doi:10.1029/94PA00208.

Tisserand, A., B. Malaizé, E. Jullien, S. Zaragosi, K. Charlier, and F. Grousset (2009), African monsoon enhancement during the penultimate glacial period (MIS 6.5 ~ 170 ka) and its atmospheric impact, *Paleoceanography*, *24*, PA2220, doi:10.1029/2008PA001630.

Van Camp, L., L. Nykjaer, E. Mittelstaedt, and P. Schlittenhardt (1991), Upwelling and boundary circulation off Northwest Africa as depicted by infrared and visible satellite observations, *Prog. Oceanogr.*, *26*(4), 357–402, doi:10.1016/0079-6611(91)90012-B.

Volbers, A. N. A., and R. Henrich (2004), Calcium carbonate corrosiveness in the South Atlantic during the Last Glacial

Maximum as inferred from changes in the preservation of Globigerina bulloides: A proxy to determine deep-water circulation patterns?, *Mar. Geol.*, *204*, 43–57, doi:10.1016/S0025-3227(03)00372-4.

Weaver, B. L., D. A. Wood, J. Tarney, and J. L. Joron (1987), Geochemistry of ocean island basalts from the South Atlantic: Ascension, Bouvet, St. Helena, Gough and Tristan da Cunha, in *Alkaline Igneous Rocks*, edited by J. G. Fitton and B. G. J. Upton, *Geol. Soc. Spec. Publ.*, *30*, 253–267, doi:10.1144/GSL.SP.1987.030.01.11.

Weltje, G. J., and R. Tjallingii (2008), Calibration of XRF core scanners for quantitative geochemical logging of sediment cores: Theory and application, *Earth Planet. Sci. Lett.*, *274*(3–4), 423–438, doi:10.1016/j.epsl.2008.07.054.

Wien, K., D. Wissmann, M. Kölling, and H. D. Schulz (2005), Fast application of X-ray fluorescence spectrometry aboard ship: How good is the new portable Spectro Xepos analyser?, *Geo Mar. Lett.*, *25*(4), 248–264, doi:10.1007/s00367-004-0206-x.

Wilke, B. M., B. J. Duke, and W. L. O. Jimoh (1984), Mineralogy and chemistry of harmattan dust in Northern Nigeria, *Catena*, *11*(1), 91–96, doi:10.1016/S0341-8162(84)80009-0.

Yarincik, K. M., R. W. Murray, and L. C. Peterson (2000), Climatically sensitive eolian and hemipelagic deposition in the Cariaco Basin, Venezuela, over the past 578,000 years: Results from Al/Ti and K/Al, *Paleoceanography*, *15*(2), 210–228, doi:10.1029/1999PA900048.

Zabel, M., T. Bickert, L. Dittert, and R. R. Haese (1999), Significance of the sedimentary Al/Ti ratio as an indicator for variations in the circulation patterns of the equatorial North Atlantic, *Paleoceanography*, *14*(6), 789–799, doi:10.1029/1999PA900027.

Zabel, M., R. R. Schneider, T. Wagner, A. T. Adegbie, U. de Vries, and S. Kolonic (2001), Late Quaternary climate changes in Central Africa as inferred from terrigenous input to the Niger Fan, *Quat. Res.*, *56*(2), 207–217, doi:10.1006/qres.2001.2261.

Zwolsman, J. J. G., and G. T. M. van Eck (1999), Geochemistry of major elements and trace metals in suspended matter of the Scheldt estuary, southwest Netherlands, *Mar. Chem.*, *66*(1–2), 91–111, doi:10.1016/S0304-4203(99)00026-2.